MOLECULAR AND CELLULAR BIOLOGY, Nov. 2004, p. 9968–9985 Vol. 24, No. 22
0270-7306/04/$08.00+0 DOI: 10.1128/MCB.24.22.9968–9985.2004

Xenopus Cds1 Is Regulated by DNA-Dependent Protein Kinase and ATR during the Cell Cycle Checkpoint Response to Double-Stranded DNA Ends

Troy D. McSherry[1,2] and Paul R. Mueller[1,3]*

Center for Molecular Oncology,[1] Department of Biochemistry and Molecular Biology,[2] and Department of Molecular Genetics and Cell Biology and Committees on Developmental Biology, Cancer Biology, and Genetics,[3] University of Chicago, Chicago, Illinois

Received 26 April 2004/Returned for modification 7 June 2004/Accepted 30 August 2004

The checkpoint kinase Cds1 (Chk2) plays a key role in cell cycle checkpoint responses with functions in cell cycle arrest, DNA repair, and induction of apoptosis. Proper regulation of Cds1 is essential for appropriate cellular responses to checkpoint-inducing insults. While the kinase ATM has been shown to be important in the regulation of human Cds1 (hCds1), here we report that the kinases ATR and DNA-dependent protein kinase (DNA-PK) play more significant roles in the regulation of *Xenopus* Cds1 (XCds1). Under normal cell cycle conditions, nonactivated XCds1 constitutively associates with a *Xenopus* ATR complex. The association of XCds1 with this complex does not require a functional forkhead activation domain but does require a putative SH3 binding region that is found in XCds1. In response to double-stranded DNA ends, the amino terminus of XCds1 is rapidly phosphorylated in a sequential pattern. First DNA-PK phosphorylates serine 39, a site not previously recognized as important in Cds1 regulation. *Xenopus* ATM, ATR, and/or DNA-PK then phosphorylate three consensus serine/glutamine sites. Together, these phosphorylations have the dual function of inducing dissociation from the ATR complex and independently promoting the full activation of XCds1. Thus, the checkpoint-mediated activation of XCds1 requires phosphorylation by multiple phosphoinositide 3-kinase-related kinases, protein-protein dissociation, and autophosphorylation.

During the eukaryotic cell cycle, distinct biochemical processes such as DNA replication and cell division must be coordinated to ensure integrity of the genome. Genomic insults resulting from both external and internal events are constantly disrupting these essential processes and placing cell duplication at risk. Consequently, organisms have developed cell cycle checkpoints, elaborate signal transduction pathways that monitor for atypical cell cycle progression. For example, in the event of DNA damage, the DNA damage checkpoint induces a cell cycle arrest while simultaneously activating either DNA repair or apoptotic pathways (14, 55). Defects in the DNA damage checkpoint system allow for continued cell division in the presence of damaged or unreplicated DNA, leading to genomic instability (61).

Phosphoinositide 3-kinase-related kinases (PIKKs) are principal components of the DNA damage checkpoint pathway (1). These proteins are characterized by their large size (>200 kDa) and by the presence of a highly conserved phosphoinositide 3-kinase-like catalytic domain. In addition, although these kinases contain a putative lipid kinase domain, they appear to function principally as protein kinases (1). Checkpoint-associated PIKKs are conserved in all eukaryotic organisms from yeast to humans. In the yeasts *Schizosaccharomyces pombe* and *Saccharomyces cerevisiae*, Rad3 and Mec1 have been shown to be essential for checkpoint induction after UV, ionizing radiation, and DNA replication blocks (12). In metazoans, the PIKKs ATR, ATM, and DNA-dependent protein kinase (DNA-PK) play multiple, possibly redundant roles during a checkpoint response. ATM is involved in the checkpoint response to ionizing radiation, while ATR seems to play a primary role in checkpoints induced by UV irradiation or DNA replication blocks (59). DNA-PK, which has essential functions in V(D)J recombination, as well as in nonhomologous end joining, is also associated with the checkpoint response (59).

In addition to the PIKKs, two downstream kinase families have been implicated as playing important functions in the checkpoint pathway. These are the checkpoint kinases Chk1 and Cds1 (Chk2). In fission yeast, Chk1 is essential for G_2/M checkpoint induction in the event of DNA damage, while Cds1 is involved in checkpoint activation following replication blocks (45). Both Chk1 and Cds1 phosphorylate Cdc25C, a mitotic phosphatase required for entry into mitosis. This phosphorylation both inhibits Cdc25 activity directly and allows for the binding of 14-3-3 proteins, leading to relocalization of Cdc25 out of the nucleus (45). Chk1 and Cds1 have also been linked with the checkpoint-dependent stabilization of Mik1, a Wee-like kinase involved in the maintenance of G_2 phase (45). Cds1 and Chk1 function in a similar manner in metazoans (6, 40). In mammalian cells, Chk1 and Cds1 have been shown to play roles in modulating the functions of cell cycle and cell cycle checkpoint proteins Cdc25A, Cdc25C, p53, and BRCA1 (6, 40). Furthermore, Cds1 targets p53 and other factors involved in the induction of the apoptotic pathway (49, 60).

We are particularly interested in understanding the regulation of Cds1 activity during cell cycle checkpoints. Members of the Cds1 family are serine/threonine kinases that typically consist of three distinct domains: an amino-terminal SQ/TQ clus-

* Corresponding author. Mailing address: Center for Molecular Oncology, University of Chicago, JFK R318, 924 E. 57th St., Chicago, IL 60637. Phone: (773) 834-0909. Fax: (773) 702-4394. E-mail: pmueller@midway.uchicago.edu.

ter domain (SCD), a central forkhead activation (FHA) domain, and a carboxyl-terminal kinase domain (6). The SCD is named for the presence of multiple serine-glutamine and/or threonine-glutamine (SQ/TQ) motifs that are possible phosphorylation sites preferred by the checkpoint-activated PIKKs ATM, ATR, and DNA-PK (1). The SCD of human Cds1 (hCds1) possesses a total of seven such sites, several of which are phosphorylated during a checkpoint response. Although the function of many of these SQ/TQ phosphorylations remains unclear, the phosphorylation of a particular site, threonine 68, is essential for hCds1 checkpoint-mediated activation and for the interaction of Cds1 with other factors during the checkpoint response (4, 37, 39, 41). The FHA domain is also required for hCds1 kinase function, and mutations in this region have been linked to a variant form of Li-Fraumeni syndrome and to some forms of colon cancer (7, 15, 35). Structural studies have shown that the hCds1 FHA domain has a strict binding preference for phosphorylated threonine residues (36). Accordingly, there have been several reports suggesting that the checkpoint-mediated activation of hCds1 is the result of Cds1/Cds1 dimerization that is governed by the binding of the FHA domain from one Cds1 molecule to phosphorylated threonine 68 of a second Cds1 molecule (2, 3, 58). This dimerization promotes the subsequent phosphorylation of key residues in the kinase domain of hCds1, leading to complete kinase activation (33). The checkpoint-induced phosphorylations and activation of the Cds1 family of kinases are accompanied by a gel mobility shift on sodium dodecyl sulfate-polyacrylamide gel electrophoresis (SDS-PAGE) gels (9, 10, 20, 38).

In mammals, regulation of Cds1 has been linked primarily to the activity of ATM. In particular, ATM has been shown to be essential for the activation of hCds1 in response to ionizing radiation, directly phosphorylating hCds1 on threonine 68 (4, 10, 37–39, 41). ATR, on the other hand, has been linked chiefly with Chk1, activating Chk1 after UV irradiation-induced DNA damage and after DNA replication inhibition (59). Although ATR can phosphorylate hCds1 in vitro (39), it has yet to be linked with hCds1 regulation in vivo. However, hCds1 does become activated in ATM-deficient cell lines and in ATM-independent checkpoints induced by UV irradiation and DNA replication inhibition, suggesting that PIKKs besides ATM may be involved in hCds1 activation (10, 24, 38, 52). In *S. cerevisiae*, the ATR homolog Mec1 has been shown to phosphorylate the checkpoint protein Rad9, which then appears to function as a scaffold for the binding and autophosphorylation of Rad53, the *S. cerevisiae* Cds1 homolog (53). Potential Rad9 homologs found in *S. pombe*, Mrc1, and mammals, BRCA1, p53 binding protein 1, and Mdc1, have all been shown to interact with Cds1 and to regulate its function (34, 37, 51, 56). However, it is unclear whether these proteins play a scaffolding role during Cds1 activation.

Interestingly, although phosphorylation of threonine 68 appears to play a central role in Cds1 activation in mammals, this residue is not conserved in Cds1 homologs that are found in *Xenopus* and other species. In fact, *Xenopus* Cds1 (XCds1) does not possess any TQ motifs, sites that could perform the FHA binding and dimerization functions that are mediated by the hCds1 phosphothreonine 68 epitope (20). Despite the absence of a site equivalent to threonine 68, XCds1 is regulated in a checkpoint-dependent manner (20, 27), suggesting that Cds1 is regulated differently in humans and *Xenopus*.

The *Xenopus* cell-free egg extract system has been effectively used to examine various aspects of cell cycle checkpoints, including the roles of Chk1 and Cds1 in checkpoint responses (20, 31, 50). In this study, we used this system to examine the regulation of XCds1 and the role that the PIKKs play in this regulation. We found that a complex exists in *Xenopus* extracts that contains *Xenopus* ATR (XATR) and XCds1. This complex is disrupted upon the induction of specific XCds1-activating checkpoints. In addition, we found that an early step in the checkpoint-mediated activation of XCds1 is the phosphorylation of a non-SQ site (serine 39) by DNA-PK. XCds1 is subsequently phosphorylated on its three SQ sites by ATM, ATR, and/or DNA-PK, and together these modifications promote the dissociation of XCds1 from the XATR complex. Mutant forms of XCds1 that lack these PIKK phosphorylation sites fail to dissociate from XATR and are defective in the ability to become activated during a checkpoint response. Finally, we found that disruption of the putative FHA domain in XCds1 does not disrupt the association of XCds1 with XATR. Instead, a predicted SH3 binding domain is required for this association. In sum, our results indicate that XCds1 is regulated through protein-protein interactions and through phosphorylation by multiple checkpoint PIKKs during cell cycle checkpoints.

MATERIALS AND METHODS

Antibodies. Recombinant XATR (amino acids 2351 to 2654) (21, 22), *Xenopus* ATM (XATM; amino acids 1066 to 1224, based on a partial cDNA) (46), and XCds1 (amino acids 1 to 197; GenBank accession no. AAG59884) (18, 20) were used to immunize rabbits and generate antisera (Covance Research Products, Inc., Denver, Pa.). Anti-XATR and anti-XATM antibodies were purified from the respective antiserum by affinity chromatography against the immunizing antigen, and the anti-XCds1 antibodies were purified by affinity chromatography against the first 86 amino acids of XCds1 as previously described (42). Rabbit polyclonal antibodies were also generated against the carboxyl-terminal peptide (CTP) of XATR (EATDENLLSQMYLGWAPYM; Zymed Laboratories Inc., San Francisco, Calif.) and purified against the immunizing peptide or recombinant XATR (amino acids 2351 to 2654) as previously described (42). This XATR CTP antibody was used to immunoprecipitate XATR in coimmunoprecipitation experiments, while the XATR (2351 to 2654) antibody was used for Western blotting and to immunoprecipitate XATR for kinase assays. Additional antibodies used were anti-Myc (Ab-1, clone 9E10; Calbiochem-Novabiochem Corp., San Diego, Calif.), anti-glutathione *S*-transferase (anti-GST) (Z-5; Santa Cruz Biotechnology, Santa Cruz, Calif.), anti-Flag (Sigma-Aldrich Corp., St. Louis, Mo.), and anti-Ku70 (N3H10; Covance Research Products, Inc.). Western blotting was performed as previously described (42). Commercial antibodies were used as described by the manufacturers.

Expression plasmids. Full-length XCds1 (matching the sequence with GenBank accession no. AAG59884) was amplified from a *Xenopus* oocyte library (11) via PCR. The XCds1 35-517 and 87-517 deletion mutant forms were prepared by amplifying the appropriate fragments from this construct. The XCds1 3AQ (S10A, S13A, S29A), N324A, and R117W mutant forms were prepared via PCR-directed mutagenesis as previously described (23). The XCds1 S39A, 4A (S10A, S13A, S29A, S39A), P55A, 4A P55A, 6A (S10A, S13A, S29A, S39A, T355A, T359A), and 2TA (T355A, T359A) mutant forms were prepared via the QuikChange site-directed mutagenesis kit as described by the manufacturer (Stratagene, La Jolla, Calif.). Full-length XCds1 and all XCds1 derivatives and mutant forms were subcloned into pCS2+ (54) and sequenced for accuracy.

The pCS2+XCds1 constructs were either used directly to produce ^{35}S-labeled recombinant XCds1 as previously described (42) or subcloned into a modified pET28a vector (Calbiochem-Novabiochem Corp.) to create versions of the appropriate XCds1 constructs that have both a 5′ six-His tag and a 3′ Flag tag for protein expression (see below). The various GST-XCds1 N86 constructs were prepared by amplifying the fragment encoding the first 86 amino acids of the appropriate XCds1 pCS2+ plasmids. These fragments were then cloned into pGEX 4T2 to create pGEX 4T2 XCds1 N86 and derivatives and sequenced for

accuracy. To prepare pFastBac HT-XCds1-Myc, XCds1 was amplified via PCR and subcloned into pCS2+MT (54) to create a 3′ Myc-tagged version of XCds1. The XCds1-Myc fragment was then subcloned into pFastBac HTc (Invitrogen Corp., Carlsbad, Calif.) to create pFastBac HT-XCds1-Myc with a 5′ six-His tag and a 3′ Myc tag and sequenced for accuracy. To create pGEX 4T2 Xp53 N39, *Xenopus* p53 (Xp53; GenBank accession no. AAC60746) was amplified from a *Xenopus* cDNA library (11) via PCR. This construct was subsequently used to amplify a fragment encoding the first 39 amino acids of Xp53, which was subcloned into pGEX 4T2 (Pharmacia) to create a GST-Xp53 fusion protein. This construct was sequenced for accuracy. pGEX 4T2 XCdc25C (amino acids 254 to 316) was prepared as previously described (20). pGEX 2T hCds1 N92-WT and -T68A were gifts from Clare McGowan.

Recombinant protein production and purification. The various recombinant H6-XCds1-Flag, GST-XCds1 N86, GST-hCds1 N92, GST-XCdc25, and GST-Xp53 N39 proteins were produced in the Rossetta *E. coli* strain (Calbiochem-Novabiochem Corp.) from the appropriate pET 28a-Flag XCds1, pGEX 4T2 XCds1 N86, pGEX 4T2, pGEX 2T hCds1 N92, pGEX 4T2 XCdc25C, and pGEX 4T2 Xp53 N39 constructs as suggested by the manufacturers, except that induction was at 25°C and for 50 min (all pET 28a-Flag XCds1 constructs; *pET System Manual* [Calbiochem-Novabiochem Corp.]) or for 1 h (all pGEX constructs; *GST Gene Fusion System Handbook* [Amersham Biosciences Corp., Piscataway, N.J.]). Briefly, recombinant H6-XCds1-Flag lysates were prepared by resuspending the cells in lysis buffer (50 mM $NaHPO_4$ [pH 7.6], 300 mM NaCl, 0.5% Triton X-100, 10 mM imidazole, 5 mM EGTA, 1 mM phenylmethylsulfonyl fluoride [PMSF]), followed by sonication on ice. The lysates were clarified by centrifugation, and the resulting supernatant was bound to Ni-iminodiacetic acid beads as previously described (30, 42). The bound beads were washed three times with 10 bed volumes of lysis buffer modified to contain 500 mM NaCl. The purified XCds1 proteins were eluted from the beads with elution buffer (25 mM HEPES [pH 7.5], 150 mM NaCl, 250 mM imidazole, 1 mM PMSF, PCL protease inhibitors [10 μg each of pepstatin, chymostatin, and leupeptin/ml]) and then dialyzed against 10 mM HEPES (pH 7.6)–150 mM NaCl and then quantified and stored at −80°C until use. The recombinant GST-XCds1 N86, GST-hCds1 N92, GST-XCdc25, and GST-Xp53 N39 proteins were prepared as described for H6-XCds1-Flag purification except that cells were resuspended in 1× phosphate-buffered saline (137 mM NaCl, 2.7 mM KCl, 4.3 mM Na_2HPO_4, containing 1.4 mM KH_2PO_4, 1 mM PMSF purified on glutathione beads (Amersham Biosciences Corp.), and eluted with 10 mM glutathione (Sigma-Aldrich Corp.) as described by the manufacturer (*GST Gene Fusion System Handbook* [Amersham Biosciences Corp.]). Recombinant H6-XCds1-Myc was produced in Sf9 insect cells and purified by nickel column chromatography as previously described (30, 42).

***Xenopus* egg extracts, shifting assays, and coimmunoprecipitations.** Normal *Xenopus* egg cell cycle cytostatic factor extracts (mitotic or interphase) or aphidicolin-induced checkpoint extracts were prepared as previously described (42, 43). Single-stranded DNA (ssDNA) checkpoints were induced by adding PhiX virion ssDNA (New England Biolabs, Beverly, Mass.) to a final concentration of 50 ng/μl. Double-stranded DNA (dsDNA) end checkpoints were prepared by adding plasmid DNA that was predigested with HpaII (29 cleavage sites per plasmid) to a final concentration of 30 to 50 ng of DNA/μl. After the addition of DNA, interphase and checkpoint-induced extracts were activated (cycled) by the addition of $CaCl_2$ (0.4 mM) and incubation at 22°C for the indicated time before being processed. Where indicated, wortmannin was added to 100 μM prior to $CaCl_2$ activation. Mitotic extracts were kept on ice without $CaCl_2$ addition for the indicated time before being processed. Unless noted otherwise, extracts were supplemented with cycloheximide (CHX; 100 μg/μl) to block entry into mitosis after interphase.

The total-extract samples used for shift analysis were 2 μl of the extract taken at the indicated time, frozen on dry ice, and stored at −80°C until needed. For the samples treated with lambda phosphatase, 2 μl of extract was taken at the indicated time, diluted to a final volume of 50 μl containing 1× lambda phosphatase buffer, 2 mM $MnCl_2$, and 200 U of lambda phosphatase (New England Biolabs), and then incubated at 30°C for 30 min. The reaction was terminated by addition of SDS-PAGE sample buffer and processing on a 10% gel.

In the experiments in which the shifting and/or association of ^{35}S-labeled recombinant XCds1 was examined in nondepleted extracts, a 5% volume of the appropriate ^{35}S-labeled XCds1 preparation was added 10 min prior to $CaCl_2$ activation. In the experiments in which GST-XCds1 N86 fusion proteins were added to the extracts, recombinant protein was added to the extracts to a final concentration of 5 to 10 ng/μl 10 min prior to $CaCl_2$ activation. In the experiments in which the shifting and/or association of ^{35}S-labeled recombinant XCds1 were examined in XCds1-depleted extracts, extracts were depleted of endogenous XCds1 (see below) before activation or any other modification (addition of DNA, proteins, CHX, wortmannin, or $CaCl_2$). In these depletion–add-back experiments, the appropriate recombinant XCds1 was then added to a final concentration of 2 ng/μl along with a 5% volume of the appropriate ^{35}S-labeled XCds1 preparation 10 min prior to $CaCl_2$ activation. In the experiments in which the shifting of GST-Xp53 N39, GST-XCds1 N86, or ^{35}S-labeled XCds1 was examined in Ku-depleted extracts, extracts were depleted of endogenous Ku (see below) before activation or any other modification (addition of DNA, proteins, CHX, wortmannin, or $CaCl_2$). Either GST-Xp53 N39 was then added to a final concentration of approximately 20 ng/μl or GST-XCds1 N86 or ^{35}S-labeled XCds1 was added as described above 10 min prior to $CaCl_2$ activation.

For Myc-tagged XCds1 coimmunoprecipitation experiments, recombinant H6-XCds1-Myc was added to the egg extracts at a final concentration of 2.5 ng/μl 10 min prior to $CaCl_2$ activation. Both ATR and Myc-tagged XCds1 coimmunoprecipitations were performed after the extracts had been incubated for the indicated time, or for 90 min if not noted otherwise, and after the total-extract samples had been taken. Two hundred microliters of the extracts was moved to ice and made 0.3% NP-40. Next, the extracts were precleared by rotation for 20 min at 4°C in the presence of 1 μg of nonspecific antibody (rabbit anti-mouse immunoglobulin G [IgG; ICN Pharmaceuticals, Inc., Aurora, Ohio] for the XATR immunoprecipitations or goat anti-mouse IgG [ICN Pharmaceuticals, Inc.] for the Myc immunoprecipitations) and 10 μl of swelled protein A beads (Sigma-Aldrich Corp.). After removal of the clearing beads, the precleared extracts were rotated for 1.5 h at 4°C in the presence of the immunoprecipitating antibody: 5 to 10 μg of anti-XATR CTP antibody (XATR immunoprecipitation), 2 μg of anti-Myc antibody (Myc-XCds1 immunoprecipitation), 5 to 10 μg of rabbit anti-mouse IgG (control immunoprecipitation for XATR immunoprecipitations), or 2 μg of goat anti-mouse IgG (control immunoprecipitation for Myc immunoprecipitations). After binding the primary antibody, 10 μl of swelled protein A beads (for anti-XATR or rabbit control) or protein G beads (Pierce Biotechnology Inc., Rockford, Ill.) (for anti-Myc or mouse control) was added, and the reaction mixtures were rotated for an additional 1 h at 4°C. The immunoprecipitated proteins bound to beads were washed three times with 1 ml of IP wash buffer A (25 mM HEPES [pH 7.5], 0.45% NP-40, 25 mM NaF, 1 mM $NaOVO_4$, 50 mM β-glycerol phosphate, 14 mM EGTA, 10 mM $MgCl_2$) and then resuspended in SDS-PAGE sample buffer and immediately processed for SDS–7% PAGE.

XCds1 and Ku immunodepletion. Endogenous XCds1 was depleted from 600 μl of nonactivated (mitotic) egg extract by two consecutive rounds of immunodepletion. Briefly, anti-XCds1 antibody–protein A beads were prepared by binding 40 μg of anti-XCds1 antibodies to 75 μl of swelled protein A beads for 1 h at 4°C with rotation. For mock depletion controls, 40 μg of rabbit anti-mouse IgG was used in place of the anti-XCds1 antibody. The antibody-protein A beads were then added to the extract, and the extract was rotated for 35 min at 4°C. The beads were removed, and the extract was subjected to a second round of depletion. After the second depletion, any free anti-XCds1 or control antibody remaining in the extracts was removed by three consecutive washes (with rotation for 12 min each time at 4°C) with 20 μl of swelled protein A beads.

Endogenous *Xenopus* Ku70 was depleted from 50 μl of nonactivated (mitotic) egg extract by two consecutive rounds of immunodepletion. Briefly, anti-Ku70 antibody–protein G beads were prepared by binding 25 μl of anti-Ku70 antibodies (Covance N3H10; Covance Research Products, Inc.) to 25 μl of swelled protein G beads for 1 h at 4°C with rotation. For mock depletion controls, 20 μg of goat anti-mouse IgG (ICN Pharmaceuticals, Inc.) was used in place of the anti-Ku70 antibody. The antibody-protein G bead mixture was then added to the extract, and the extract was rotated for 40 min at 4°C. The beads were removed, and the extract was subject to a second round of depletion. After the second depletion, any free anti-Ku70 or control antibody remaining in the extracts was removed by a wash (with rotation for 12 min at 4°C) with 25 μl of swelled protein G beads.

Immunoprecipitation of recombinant XCds1 for kinase assays. XCds1 depletion–add-back extracts were prepared as described above and incubated at 22°C for 75 min, and then recombinant XCds1 was recovered by immunoprecipitation after the total-extract samples had been taken. One hundred microliters of the extracts was moved to ice and made 0.5% NP-40. Next, the extracts were rotated for 1 h at 4°C in the presence of the immunoprecipitating antibody, 5 to 10 μg of anti-Flag M2 (Sigma-Aldrich Corp.). After binding of the primary antibody, 10 μl of swelled protein G beads was added and the reaction mixtures were rotated for an additional 1 h at 4°C. The immunoprecipitated proteins bound to beads were washed once with 1 ml of IP wash buffer B (25 mM HEPES [pH 7.5], 150 mM NaCl, 0.5% NP-40, 25 mM NaF, 1 mM $NaOVO_4$, 50 mM β-glycerol phosphate, 14 mM EGTA, 10 mM $MgCl_2$, 1 mM PMSF, PCL protease inhibitors) containing 1 μM microcystin, twice with IP wash buffer B, and twice with XCDs1 kinase buffer (10 mM Tris [pH 7.5], 10 mM $MgCl_2$, 1 mM dithiothreitol [DTT]) containing 1 mM PMSF and PCL protease inhibitors. Immunoprecipi-

tates (IPs) were resuspended in 100 μl of kinase buffer and processed immediately for kinase assays (see below). In addition, in all cases 25 μl of the resuspended IP was treated with lambda phosphatase (as described above) and then subsequently subjected to anti-XCds1 Western blotting to confirm equal recovery of recombinant XCds1.

Immunoprecipitation of XATR and XATM for kinase assays. XATR and XATM were immunoprecipitated from *Xenopus* mitotic extracts (see above). One hundred microliters of extract was diluted with 700 μl of dilution buffer (50 mM Tris [pH 7.5], 150 mM NaCl, 1% Tween 20, 0.3% NP-40, 1 mM NaF, 1 mM $NaOVO_4$, PCL protease inhibitors). The diluted extract was precleared by adding 1 μg of rabbit anti-mouse IgG and 75 μl of diluted protein A beads (20% slurry of protein A beads preswelled in dilution buffer) and then rotating the extract for 30 min at 4°C. After removal of the clearing protein A beads, 3 μg of either anti-XATR (2351-2654) or anti-XATM antibody was added to the precleared extract, followed by rotation at 4°C for 2 h. A 75-μl volume of diluted protein A beads was then added, followed by rotation for an additional 1 h at 4°C. XATR- or XATM-bound beads were recovered and washed once with 1 ml of Dilution Buffer, twice with 1 ml of dilution buffer containing 500 mM LiCl, and twice with 1 ml of ATR/ATM kinase buffer (20 mM HEPES [pH 7.5], 50 mM NaCl, 10 mM $MgCl_2$, 10 mM $MnCl_2$, 1 mM DTT) with PCL protease inhibitors added. The washed beads were resuspended in 50 μl of kinase buffer and used immediately.

In vitro kinase assays. For XCds1 basal kinase assays, 200-μg samples of the various recombinant H6-XCds1-Flag proteins were incubated with 1 μg of GST-XCdc25 (amino acids 254 to 316) in XCds1 kinase buffer (10 mM Tris [pH 7.5], 10 mM $MgCl_2$, 1 mM DTT), containing 10 μM ATP and 10 μCi of [γ-^{32}P]ATP in a final volume of 50 μl for 20 min at 22°C before termination by the addition of SDS-PAGE sample buffer and immediate processing for SDS–10% PAGE to visualize both the XCds1 autophosphorylation product and the phosphorylated XCdc25 substrate.

To measure the activation of XCds1 during the checkpoint response, recombinant XCds1 was recovered after treatment in interphase of checkpoint extracts (see above) and then kinase assays were performed in a final volume of 50 μl (diluted with XCds1 kinase buffer) containing 10 μl of the H6-XCds1-Flag IP slurry, 1 μg of GST-XCdc25 (amino acids 254 to 316), 10 μCi of [γ-^{32}P]ATP, and 10 μM ATP. The reaction mixtures were rotated for 20 min at 22°C before termination of the reactions by addition of SDS-PAGE sample buffer and immediate processing for SDS–10% PAGE.

XATR and XATM kinase assays were performed in a final volume of 50 μl (diluted with ATR/ATM kinase buffer) containing 25 μl of the XATR or XATM IP slurry, the indicated Cds1 substrate, 10 μCi of [γ-^{32}P]ATP, and 10 μM ATP. The reaction mixtures were rotated for 30 min at 22°C before termination by the addition of SDS-PAGE sample buffer and immediate processing for SDS–8 to 12% step PAGE.

For DNA-PK kinase assays, 20 U of DNA-PK (Promega Corp., Madison, Wis.) was incubated in a 50-μl reaction mixture with DNA-PK kinase buffer (50 mM HEPES [pH 7.5], 100 mM KCl, 10 mM $MgCl_2$, 0.2 mM EGTA, 0.1 mM EDTA, 1 mM DTT), 200 ng of sheared salmon sperm, 4 μg of bovine serum albumin, 200 μM ATP, 15 μCi of [γ-^{32}P]ATP, and the indicated XCds1 substrate for 30 min at 30°C. Reactions were terminated by the addition of SDS-PAGE sample buffer and immediate processing for SDS–10% PAGE.

RESULTS

The constitutive association between XATR and XCds1 is disrupted under checkpoint conditions that activate XCds1. In humans, Cds1 (hCds1/Chk2) has been shown to associate with a variety of cell cycle checkpoint proteins, including BRCA1, p53 binding protein 1, and Mdc1 (34, 37, 56). Given that checkpoint PIKKs have been shown to play an essential role in checkpoint-mediated hCds1 activation, we were interested in determining whether XCds1 and checkpoint PIKKs also associate. We added recombinant, Myc-tagged XCds1 protein to *Xenopus* mitotic extracts and recovered the recombinant XCds1 by anti-Myc immunoprecipitation. Western blotting of anti-Myc IPs indicated that XATR, but not XATM, associates with recombinant XCds1 in *Xenopus* egg extracts (Fig. 1A; data not shown). To confirm these results, we performed the reciprocal experiment: immunoprecipitation of endogenous XATR or XATM from noncheckpoint and checkpoint conditions, followed by blotting for the presence of endogenous XCds1. As reported previously, XCds1 displays a large molecular weight shift in extracts that are checkpoint arrested with either ssDNA or dsDNA ends, consistent with the phosphorylation and activation of XCds1 during a checkpoint response (20). In contrast, XCds1 does not shift in normal cell cycle extracts or in extracts arrested with the replication inhibitor aphidicolin, indicating a lack of activation (Fig. 1B, total extract).

These same extracts were subjected to immunoprecipitation with antibodies against XATM and XATR or with control antibodies, followed by blotting for the presence of endogenous XCds1. Consistent with the anti-Myc immunoprecipitation results, we observed that XCds1 coimmunoprecipitated with XATR under mitotic, interphase, and DNA replication checkpoint conditions (Fig. 1B, middle parts). This interaction is independent of DNA, since XCds1 coimmunoprecipitated with XATR in extracts in which no nuclei were present. Again, we were unable to identify an association between XATM and XCds1 under any of the conditions tested (data not shown). Although we were unable to detect this association, it should be noted that this is a negative result that does not formally rule out an association between XATM and XCds1. However, our positive results do establish that XATR and XCds1 associate as part of a complex in *Xenopus* egg extracts.

Interestingly, we found that the association between XCds1 and XATR was disrupted under particular cell cycle checkpoint conditions that lead to XCds1 activation, suggesting that this interaction may play a regulatory role. Whereas nonactivated XCds1 coimmunoprecipitated with XATR in DNA replication checkpoint extracts, activated XCds1 failed to coimmunoprecipitate with XATR in extracts with checkpoints induced by ssDNA or dsDNA ends (Fig. 1B). Equal amounts of XATR were immunoprecipitated under all of the extract conditions tested, indicating that the specific loss of coimmunoprecipitating XCds1 under some extract conditions was not due to differences in XATR recovery (Fig. 1B). Together, these results suggest that nonactivated XCds1 constitutively associates with XATR in *Xenopus* extracts and that this association is disrupted during specific XCds1-activating checkpoint responses.

A caveat to this interpretation is that our anti-XCds1 antibody is less effective at recognizing checkpoint-modified XCds1 from ssDNA and dsDNA extracts than it is at recognizing XCds1 from the other cell cycle extracts (Fig. 1B, total extract lanes; data not shown). To address this issue, we used radiolabeled, recombinant XCds1 as a marker of XCds1 activation and XATR association in *Xenopus* extracts. Like endogenous XCds1, ^{35}S-radiolabeled XCds1 is activated (as judged by the gel mobility shift) in a checkpoint-dependent manner (Fig. 1C, total extract). Furthermore, recombinant, radiolabeled XCds1 coimmunoprecipitated with XATR in a checkpoint-sensitive manner similar to endogenous XCds1 (Fig. 1C). Given that recombinant XCds1 behaves similarly to endogenous XCds1 in *Xenopus* extracts, we used radiolabeled, recombinant XCds1 proteins as reporters of XCds1 function in subsequent experiments.

Next, we examined the timing of XCds1 modification and dissociation during a checkpoint response. Recombinant, radiolabeled XCds1 was added to extracts either in the absence

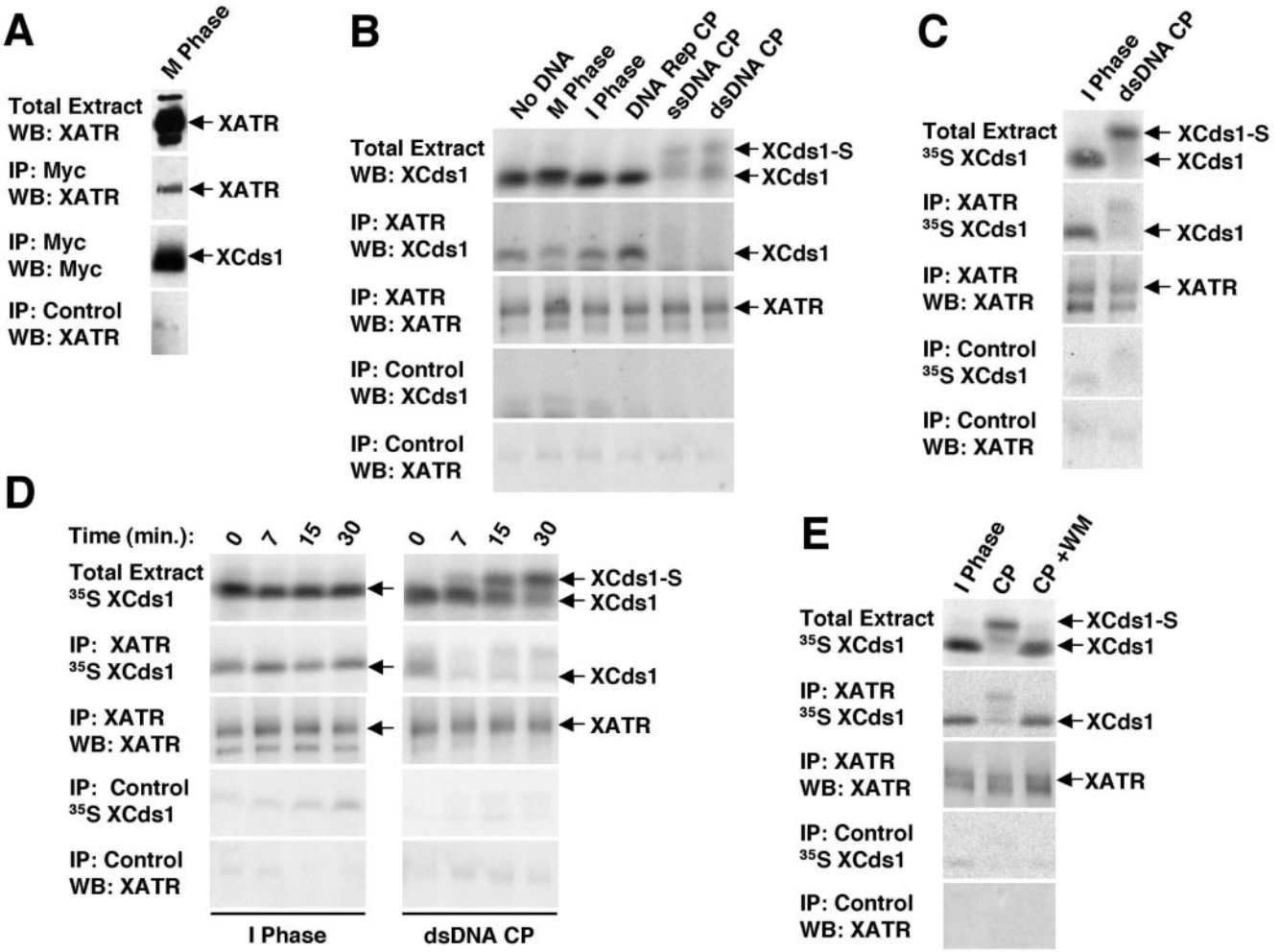

FIG. 1. XCds1 and ATR are part of a complex during the normal cell cycle but not during a checkpoint (CP) response. (A) Endogenous XATR coimmunoprecipitates with recombinant, Myc-tagged XCds1 that was added and recovered from a *Xenopus* mitotic extract. Total extract, Myc IP, and control IP were processed for Western blotting (WB) as indicated. (B) Endogenous XCds1 is modified (shifted) in extracts with CPs induced by ssDNA or dsDNA ends but not in nonperturbed mitotic (no DNA, M phase) or interphase (I phase) extracts or in extracts with CPs induced by inhibition of DNA replication. Note that only nonmodified XCds1 coimmunoprecipitates with endogenous XATR. Total extract, XATR IP, and control IP were processed for WB as indicated. Arrows indicate unshifted XCds1 (XCds1) and shifted XCds1 (XCds1-S). (C) Recombinant, ^{35}S-labeled XCds1 associates with endogenous XATR in a CP-sensitive fashion. Total extract, XATR IP, and control IP were processed for autoradiography to detect the labeled Cds1 or for WB to detect XATR. (D) The dsDNA end CP induces a rapid dissociation of ^{35}S-labeled recombinant from endogenous XATR, an interaction that is stable in normal extracts (I phase). Samples were processed at the indicated times after addition of $CaCl_2$ to the extracts either for direct SDS-PAGE and autoradiography (total extract) or for immunoprecipitation (IP) followed by autoradiography or WB. (E) The PIKK inhibitor wortmannin (WM) prevents shifting and dissociation of ^{35}S-labeled recombinant XCds1 from endogenous XATR. Interphase extracts (I phase), dsDNA CP extracts (CP), and dsDNA CP extracts containing 100 μM wortmannin (CP+WM) were prepared and processed as described for panel C.

(interphase) or in the presence of dsDNA ends (dsDNA CP). Aliquots were removed at various times after the extract began cycling (time zero) and then subjected to immunoprecipitation with either anti-XATR or control antibodies (Fig. 1D). During a checkpoint response, a significant portion of XCds1 is modified between 7 and 15 min post extract activation, as judged by the appearance of the higher-migrating form of XCds1, and by 30 min, most of the XCds1 is fully modified (total extract, Fig. 1D). As discussed below, this change in apparent molecular weight is the result of multiple phosphorylation events. The coimmunoprecipitation analysis of these same samples shows that XCds1 rapidly dissociates from XATR upon checkpoint activation (Fig. 1D, middle parts). In fact, most of the XCds1 is lost from XATR IPs as early as 7 min, regardless of whether the XCds1 is fully modified. In contrast, in the normal cell cycle extract XCds1 does not appear to be modified nor is there a change in the amount of XCds1 that coimmunoprecipitates with XATR throughout the time course of the experiment. Thus, it appears that XCds1 tightly associates with XATR under noncheckpoint conditions but then rapidly dissociates from XATR at the onset of XCds1 activation. Furthermore, the time course of the dissociation experiment suggests that complete modification of the XCds1 protein is not required for its dissociation from the XATR complex.

Because PIKK activity has been shown to be required for

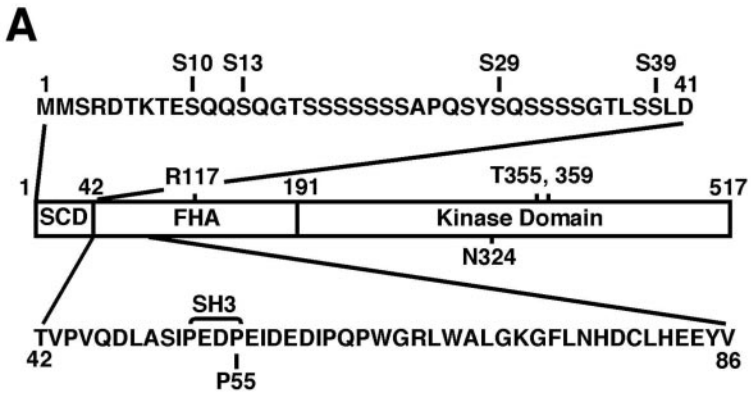

B

XCds1 Mutant	Mutation(s)	Domain
3AQ	S10A, S13A, S29A	SCD
S39A	S39A	SCD
4A	S10A, S13A, S29A, S39A	SCD
35-517	Amino-34 aa Deletion	SCD
R117W	R117W	FHA
P55A	P55A	FHA (SH3)
87-517	Amino-86 aa Deletion	SCD, FHA
4A P55A	S10A, S13A, S29A, S39A, P55A	SCD, FHA (SH3)
T2A	T355A, T359A	Kinase Activation Loop
N324A	N324A	Kinase

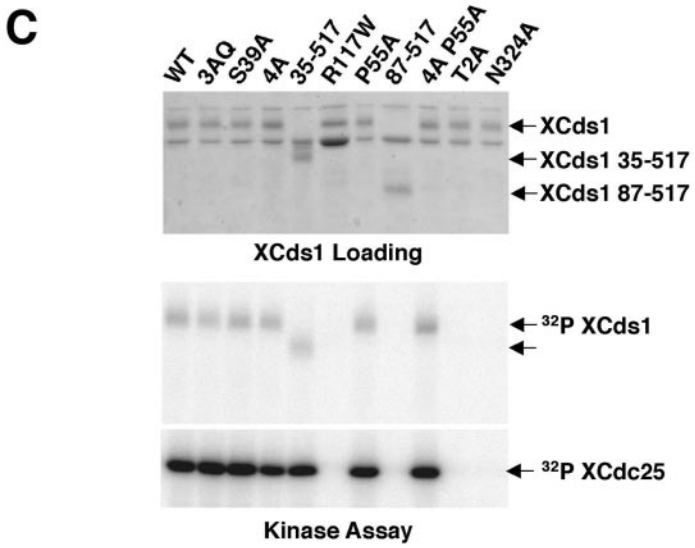

FIG. 2. Residues and regions of XCds1 analyzed in this work. (A) Schematic representing the predicted domain structure of XCds1, the predicted phosphorylation sites, and possible protein-protein interaction motifs. The boundaries of the domains were determined on the basis of the delineation of the hCds1 FHA (36). The amino terminus of XCds1 is expanded to show the SCD (residues 1 to 41) and the potential PIKK phosphorylation sites that were mutated (serines 10, 13, 29, and 39). Also expanded is the amino-terminal portion of the FHA (residues 42 to 86), which contains a putative SH3 binding domain, marked by the bracketed PEDP sequence, and the mutated proline residue (P55). Residues that were mutated in the FHA domain (residues 42 to 191) and the kinase domain (residues 192 to 517) are also indicated. (B) Table listing the various mutant forms of XCds1 used in this study along with the locations of the mutations and the domains affected. (C) In vitro kinase assays performed to measure the basal kinase activities of the various recombinant XCds1 constructs. At the top is a Coomassie-stained gel that indicates the amount of XCds1 used to measure autokinase activity (middle) or XCdc25 substrate phosphorylation activity (kinase assay, bottom).

XCds1 checkpoint-dependent activation (20), we tested whether PIKK activity is also essential for the checkpoint-dependent dissociation of XCds1 and XATR (Fig. 1E). Addition of wortmannin, a potent PIKK inhibitor, to dsDNA checkpoint extracts inhibits XCds1 activation, as determined by the loss of the XCds1 gel mobility shift (Fig. 1E, top [total extract]). Significantly, XATR immunoprecipitation under these same conditions shows that XCds1 remains in a complex with XATR (Fig. 1E, middle parts). Thus, the checkpoint-mediated dissociation of XCds1 from XATR, as well as the activation of XCds1, appears to require PIKK activity, presumably provided by one or more of the checkpoint PIKKs (ATR, ATM, or DNA-PK).

XCds1 is predicted to be a multidomain phosphoprotein. The three predicted domains of the XCds1 protein are illustrated in Fig. 2A. The overall checkpoint-dependent modification and activation of XCds1 appear to be the result of phosphorylation events: checkpoint-activated XCds1 that is subsequently treated with lambda phosphatase loses its gel mobility shift and kinase activation (20). Therefore, we reasoned that dissection of the XCds1 gel mobility shift might provide information regarding the mechanisms of XCds1 regulation. Through examination of each of the three XCds1 domains, we identified residues that may be important for the XCds1 checkpoint-dependent hyperphosphorylation and the regulation of XCds1 activity. In the amino-terminal SCD of XCds1 there are no TQ motifs but there are three SQ motifs, at serines 10, 13, and 29. These sites are putative phosphorylation sites for checkpoint PIKKs and may play a role in XCds1 regulation. Additionally, serine 39, although not an SQ/TQ site, was identified as a predicted DNA-PK phosphorylation site (44). The XCds1 FHA domain is a prime candidate for protein-protein interactions, either through self-dimerization or possibly in association with other checkpoint proteins such as XATR (3, 33, 58). Additionally, we identified a putative SH3 domain binding site (PXXP) that may also be involved in protein-protein associations (5, 10). Finally, activation of hCds1 has been shown

to require phosphorylation on two kinase domain activation loop threonines (33, 47). Phosphorylation of the analogous residues in XCds1, threonines 355 and 359, may be required for XCds1 activation. To test these possibilities, we prepared four groups of XCds1 mutants: putative PIKK phosphorylation site mutants (3AQ [S10A, S13A, S29A], S39A, 4A [3AQ, S39A], and 35-517), putative XCds1 protein-protein interaction mutants (R117W and P55A), kinase domain mutants (N324A and 2TA [T355A, T359A]), and mutants that span multiple domains (87-517 and 4A P55A) (Fig. 2B).

We first asked whether any of these mutations disrupt the basal kinase activity of XCds1 by purifying recombinant versions of these XCds1 mutants from bacteria and performing in vitro kinase assays with a fragment of XCdc25 as a substrate (Fig. 2C). Mutation of any or all of the potential PIKK phosphorylation sites (3AQ, S39A, 4A, and 35-517) and/or mutation of the putative SH3 domain binding site (P55A and 4A P55A) did not appear to significantly affect XCds1 autokinase activity (Fig. 2C, middle part) or the ability of XCds1 to phosphorylate XCdc25 (Fig. 2C, bottom part). In contrast, mutation or partial loss of the putative FHA domain (R117W and 87-517) or mutation in the kinase domain (N324A and 2TA) eliminated detectable kinase activity. Thus, while the potential PIKK phosphorylation sites may play a role in the checkpoint-mediated activation of XCds1, they are not directly required for basal XCds1 activity. Conversely, the integrity of the XCds1 FHA domain, as well as the kinase activation loop and catalytic sites, is required.

The checkpoint-dependent gel mobility shift and activation of XCds1 require autophosphorylation of XCds1 on conserved activation loop threonines. We next asked which of the putative phosphorylation sites in XCds1 are phosphorylated in cell extracts and which sites play a role in XCds1 regulation. Radiolabeled versions of various XCds1 constructs were prepared to serve as reporters of XCds1 gel mobility shifting in *Xenopus* checkpoint extracts. Initially, we added these constructs to extracts that contained endogenous XCds1. The shifting profile of the radiolabeled reporter wild-type (WT) XCds1 or kinase-dead (N324A) XCds1 is similar to that observed with endogenous XCds1, indicating that the modifications leading to XCds1 shifting can occur in *trans* (Fig. 3A, compare to Fig. 1; data not shown). In contrast, the checkpoint-induced shifting of the XCds1 T355/359A mutant (2TA) is significantly reduced. This result suggests that the XCds1 activation loop threonines are phosphorylated in a checkpoint-dependent manner and that these sites are responsible for most of the XCds1 checkpoint-dependent gel mobility shift.

It has been shown that the phosphorylation of the two activation loop threonines in hCds1 is the direct result of hCds1 kinase activity, either in *cis* or in *trans* (33, 47). To determine whether this is the case in *Xenopus*, we used immunodepletion to create a *Xenopus* extract environment devoid of endogenous XCds1 (Fig. 3B). We then added trace levels of radiolabeled XCds1 as a reporter to determine whether XCds1 activation loop threonines 355 and/or 359 could be phosphorylated in a checkpoint extract lacking XCds1 activity. In contrast to the checkpoint-dependent shifting that was observed in mock-depleted extract, in XCds1-depleted extracts, the reporter failed to undergo the degree of shifting consistent with the phosphorylation of threonines 355 and/or 359 (Fig. 3C). This result suggests that XCds1 is the principal kinase responsible for the phosphorylation of the activation loop threonines and for the ultimate activation of XCds1 in extracts. However, it is important to note that the XCds1 reporter retains a minimal degree of shifting in the depleted extracts. This minor shifting, which is wortmannin sensitive (data not shown), is reminiscent of the shifting of the XCds1 T355A, T359A mutant (2TA) during a checkpoint event (Fig. 3A). This minor shift suggests that XCds1 is still modified in checkpoint extracts even in the absence of appreciable XCds1 activity.

We next asked if we could restore complete XCds1 checkpoint-dependent shifting or activation by adding back purified recombinant XCds1 to the depleted extracts. Western blot analysis indicates that the amount of recombinant XCds1 added to the depleted extract is similar to the amount of endogenous XCds1 found in nondepleted extracts (2 ng/μl) (Fig. 3B; data not shown). The gel mobility difference between recombinant and endogenous XCds1 is the result of the added amino-terminal six-His and carboxyl-terminal Flag tags. As shown in Fig. 3C, adding back of recombinant WT XCds1, but not kinase-dead XCds1 N324A, restores most of the XCds1 gel mobility shifting in dsDNA end checkpoint extracts. Together, these results suggest that functional XCds1 is responsible for the phosphorylation of the activation loop threonines and that these posttranslational modifications are responsible for most, but not all, of the checkpoint-dependent gel mobility shift of XCds1.

To confirm that the autophosphorylation-mediated shifting of XCds1 is essential for the checkpoint-dependent activation of XCds1, we repeated the depletion–add-back experiment with either WT or kinase-dead recombinant XCds1 added to interphase or dsDNA end checkpoint extracts. We then recovered the extract-modified forms of XCds1 by anti-Flag immunoprecipitation and examined their kinase activity in vitro (Fig. 3D). As shown in Fig. 3C, WT XCds1 undergoes a major checkpoint-dependent gel mobility shift in the checkpoint extract (Fig. 3D, top, compare lanes 1 and 2). Significantly, this shift corresponds to a small but reproducible twofold activation of recombinant WT XCds1 (Fig. 3D, middle, compare lanes 1 and 2). In contrast, kinase-dead XCds1 (N324A) undergoes only the minor gel mobility shift in the checkpoint extract and exhibits background levels of kinase activity (Fig. 3D, top and middle, compare lanes 3, 4, and 5). To confirm that equal levels of recombinant XCds1 were recovered during the anti-Flag immunoprecipitation, a portion of the sample was treated with lambda phosphatase and subjected to anti-XCds1 Western analysis (Fig. 3D, bottom). Together, these results show that recombinant XCds1 can be shifted and activated in a Cds1-dependent manner in *Xenopus* cell-free checkpoint-activated extracts.

PIKKs phosphorylate the SCD of XCds1 during a checkpoint response. Having established that the major checkpoint-induced gel mobility shift of XCds1 is due to autophosphorylation on the conserved activation loop threonines (T355 and T359), we turned our attention to the minor XCds1-independent shift. We first prepared an XCds1 deletion construct in which the amino-terminal 86 residues were removed. This XCds1 87-517 construct fails to undergo any noticeable degree of checkpoint-dependent gel mobility shifting (Fig. 4A). This result, combined with the amino-terminal location of the predicted PIKK phosphorylation sites (Fig. 2A), led us to focus on the first 86 amino acids of XCds1 in our next series of experiments.

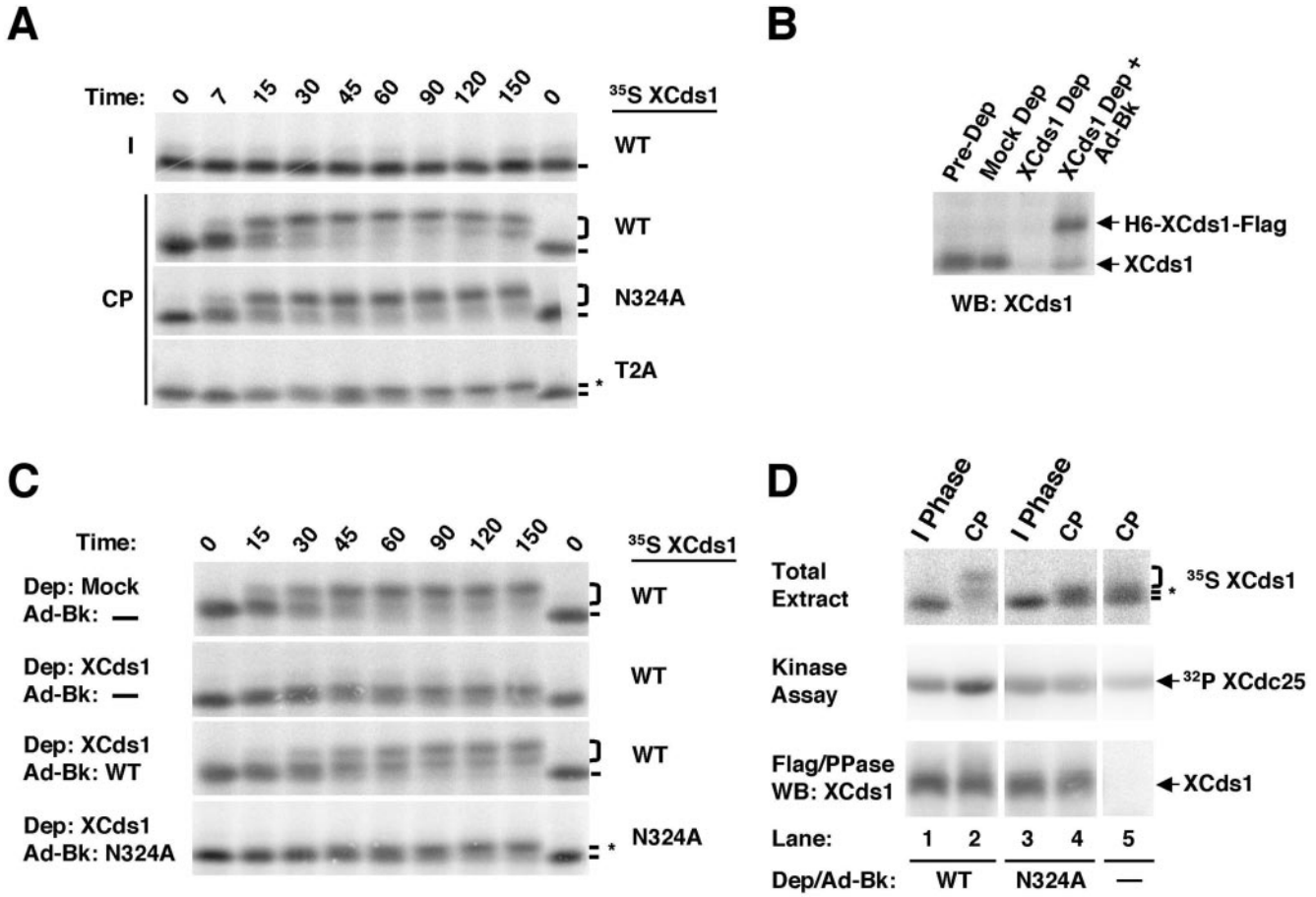

FIG. 3. Autophosphorylation of XCds1 on conserved activation loop threonines (T355 and T359) is responsible for most of the checkpoint-induced mobility shift and activation of XCds1. (A) T355 and T359 are required in *cis* for the full checkpoint-induced shift of XCds1. WT and kinase-dead (N324A) XCds1, but not kinase-dead T2A (T355A, T359A) XCds1, are modified in a WT-like manner in dsDNA end checkpoint-induced extracts. Indicated ^{35}S-labeled recombinant XCds1 proteins were added to either interphase (I) or dsDNA end-induced checkpoint (CP) extracts. Samples were processed for autoradiography at the indicated times (minutes) after the addition of $CaCl_2$. Unmodified XCds1 is indicated by a line, full shifted XCds1 is indicated by a bracket, and minor shifted XCds1 is indicated by a line with an asterisk. (B) Immunodepletion (Dep) of endogenous XCds1 and add back (Ad-Bk) of recombinant XCds1 to equivalent levels. In all cases, total extract was processed for Western blotting (WB) against anti-XCds1 antibodies. Results are shown for predepletion (Pre-Dep), after mock depletion (Mock Dep), after XCds1 depletion (XCds1 Dep), and after XCds1 depletion with the add back of recombinant H6-XCds1-Flag (XCds1 Dep + Ad-Bk). Recombinant H6-XCds1-Flag runs at a higher molecular weight than endogenous XCds1 because of the presence of amino- and carboxyl-terminal six-His and Flag tags. (C) Activated XCds1 is responsible for the full shift of XCds1 through autophosphorylation. Mock- or XCds1-depleted extracts were examined for the ability to shift an XCds1 reporter construct (^{35}S-labeled XCds1) with or without the replacement (Ad-Bk) of the depleted XCds1 with WT or kinase-dead (N324A) XCds1 to endogenous XCds1 levels (panel B; data not shown). The full checkpoint-induced XCds1 gel mobility shift (bracket) is restored by the addition of recombinant WT XCds1 but not that of kinase-dead XCds1. However, even in the absence of functional XCds1, a minor shift is observed. Samples were taken from the extracts at the indicated times and processed as described for Fig. 1D. Labels are as in panel A. (D) Recombinant WT, but not kinase-dead, XCds1 becomes activated in dsDNA end checkpoint extracts. *Xenopus* extracts were subjected to depletion of endogenous XCds1 (lanes 1 to 5) and add back of recombinant WT (lanes 1 and 2) or kinase-dead (N324A, lanes 3 and 4), Flag-tagged XCds1 or nothing (—, lane 5), as described for panels B and C. After cycling of interphase (I phase) or dsDNA end checkpoint (CP) extracts, samples were taken (total extract) and/or subjected to anti-Flag immunoprecipitation. Immunoprecipitated XCds1-Flag was then used for in vitro kinase assays with GST-XCdc25 (amino acids 254 to 316) as a substrate (kinase assay) or treated with lambda phosphatase (PPase) and then used for Western blotting (WB: XCds1).

We prepared a GST fusion protein containing the amino-terminal 86 amino acids of XCds1 (N86 WT), along with a mutant fusion protein in which all three SQ sites were mutated to AQ (N86 3AQ). These fusion proteins were added to normal or checkpoint-induced extracts for various periods of time and under different conditions (Fig. 4B). As expected, neither fusion protein is subject to a gel mobility shift under normal cell cycle conditions (Fig. 4B, lanes 1 and 2 and lanes 7 and 8). In contrast, induction of the checkpoint by dsDNA ends led to modification of both constructs; however, the degree of the gel mobility shift differs greatly (Fig. 4B, asterisks, compare lanes 4 and 10). These shifts are abolished by lambda phosphatase treatment (Fig. 4B, lanes 6 and 12), indicating that the shift-inducing modifications are phosphorylations. Additionally, these phosphorylations are wortmannin sensitive (Fig. 4B, lanes 5 and 11). Together, these shifting results suggest that the first 86 amino acids of XCds1 contains SQ and non-SQ sites that are phosphorylated during the checkpoint response by a wortmannin-sensitive kinase(s).

We performed systematic mutations of the SQ sites and

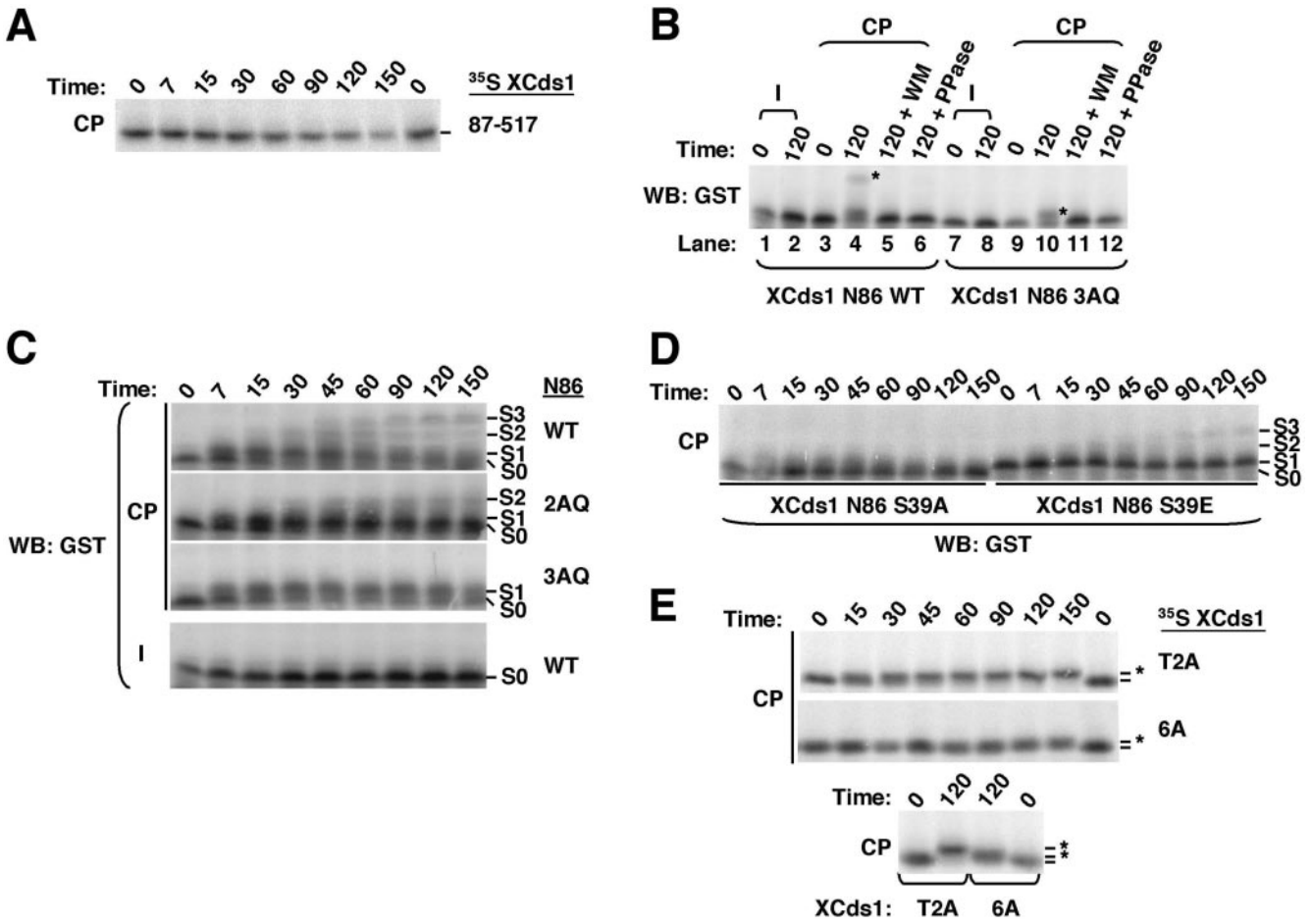

FIG. 4. XCds1 is phosphorylated on multiple PIKK sites during a checkpoint (CP) response. (A) The first 86 amino acids of XCds1 are required for all CP-induced gel mobility shifts. ^{35}S-labeled recombinant XCds1 87-517 was added to dsDNA CP extract and processed as described for Fig. 3A. (B) The amino-terminal 86 amino acids of XCds1 are phosphorylated by wortmannin (WM)-sensitive kinases on SQ and non-SQ sites during the CP response. WT GST-XCds1 N86 (WT) (lanes 1 to 6) and a mutant GST-XCds1 N86 in which all three SQ sites are mutated to alanine (3AQ) (lanes 7 to 12) were added to interphase (I) extracts (lanes 1, 2, 7, and 8), to dsDNA end CP extracts (lanes 3, 4, 9, 10), or to dsDNA end CP extracts treated with WM (lanes 5 and 11) for the indicated periods of time before being processed for Western blotting (WB) analysis with anti-GST antibodies. In lanes 6 and 12, the 120-min CP time point was treated with lambda phosphatase (PPase) before being processed for WB analysis. Asterisks indicate the shifted species. (C) A fragment comprising the amino-terminal 86 amino acids of XCds1 is phosphorylated on a non-SQ site within 7 min of CP activation and subsequently phosphorylated on multiple SQ sites during the CP response. WT GST-XCds1 N86 or mutant forms of GST-XCds1 N86 lacking two (2AQ) or three (3AQ) of the SQ sites found in XCds1 were added to interphase (I) or dsDNA end CP extracts. Samples were taken at the indicated times before being processed as described for panel B. S0 denotes the unshifted N86 fragment, while S1, S2, and S3 denote various degrees of shifting. (D) Serine 39 is required for all CP-induced phosphorylations of the N86 fragment of XCds1. Mimicking the phosphorylation of serine 39 with glutamic acid restores subsequent phosphorylations of this fragment. GST-XCds1 N86-S39A or -S39E was added to dsDNA CP extracts. Samples were processed, and the shifted species were labeled as in panel C. (E) The PIKK phosphorylation sites contribute to the minor shifting of full-length XCds1 independent of autophosphorylation. Full-length, ^{35}S-labeled recombinant XCds1 with the two activation loop threonines, T355 and T359, converted to alanine (T2A) or these same mutated sites combined with conversion of the PIKK phosphorylation sites, S10, S13, S29, S39, to alanine (6A) were added to dsDNA CP extracts and processed as for Fig. 3A. The top part shows the extended time course, while the bottom part shows an independent experiment with the 0- and 120-min samples loaded in adjacent lanes for comparison.

monitored the modification of these constructs in normal or checkpoint cell cycle *Xenopus* extracts. In dsDNA end checkpoint extracts, we found that the WT and all mutant SQ constructs underwent a similar gel migratory shift within 7 min (Fig. 4C, shift S1), approximately at the time when full-length XCds1 dissociates from the XATR-containing complex (Fig. 1D). The WT XCds1 N86 fragment (WT) then undergoes two additional shift-inducing phosphorylations (Fig. 4C, S2 and S3). In contrast, the XCds1 N86 2AQ mutant, with two of the three SQ motif serines (10 and 13) mutated to alanine, displays only one additional shift (S2). This result indicates that one of the shifts is due to phosphorylation of serine 10 and/or 13. Finally, the XCds1 N86 3AQ mutant, with all three SQ motifs mutated, undergoes only the early, 7-min, gel mobility shift.

The serine at position 39 was predicted to be a potential DNA-PK phosphorylation site (44). We empirically tested whether this site was phosphorylated in cell extracts by creating a mutant construct with this serine changed to alanine (XCds1 N86 S39A). Strikingly, mutation of this single site prevented phosphorylation of the remaining SQ sites as no appreciable shifting was observed with this XCds1 mutant fragment (Fig. 4D). This result suggests that phosphorylation of S39 may be

required for subsequent phosphorylation of the SQ sites. To test this hypothesis, we created a phosphorylation mimic at position 39 by changing the serine to glutamic acid (S39E). Although not as efficient as the WT fragment, this construct was modified and underwent the two additional mobility shifts expected from SQ phosphorylation of serines 29 and 10 and/or 13 (S2 and S3, Fig. 4D).

Finally, we asked whether phosphorylation of full-length XCds1 was dependent on these PIKK phosphorylation sites in the cell extract. Recall that most, but not all, of the full-length XCds1 checkpoint-induced shifting is caused by XCds1 autophosphorylation on T355 and T359 (Fig. 3). To test the role of the PIKK phosphorylation sites, we prepared a full-length, radiolabeled XCds1 mutant in which all six residues that we had identified as being modified during a checkpoint response (S10, S13, S29, S39, T355, and T359) were mutated to alanine (XCds1 6A). We then added this construct to *Xenopus* checkpoint extracts and compared the checkpoint-dependent shifting of this mutant with that of an XCds1 mutant with only T355 and T359 mutated (2TA). The shifting of the XCds1 6A mutant is reduced compared to that of the 2TA mutant, suggesting that phosphorylation of the amino-terminal sites contributes to the overall shifting of full-length XCds1 (Fig. 4E). However, it appears that the XCds1 6A mutant retains a minor degree of checkpoint-dependent gel mobility shifting. This retention suggests that additional sites of checkpoint-dependent XCds1 modification are yet to be identified.

Phosphorylation of the XCds1 SCD is required for XCds1 activation and dissociation from the XATR-containing complex. The wortmannin sensitivity of XCds1 shifting and dissociation (Fig. 1E) and the mutagenic analysis of XCds1 (Fig. 4) suggest that PIKK-mediated phosphorylation of the amino-terminal SCD may be required for XCds1 activation and XCds1 dissociation from the XATR-containing complex. To test this hypothesis, we created depletion–add-back extracts in which the endogenous XCds1 was depleted and replaced with equivalent levels of recombinant, full-length WT or SCD phosphorylation site mutant forms of XCds1 (Fig. 5A; data not shown). We then monitored the ability of these recombinant XCds1 proteins to undergo checkpoint-dependent gel mobility shifting, ATR dissociation, and activation (Fig. 5B and C).

The XCds1 3AQ mutant, which lacks the three SQ sites, undergoes a checkpoint-induced gel mobility shift that is almost as large as that observed with WT XCds1 (Fig. 5B, top two parts). In addition, the time courses of WT and 3AQ XCds1 shifting are similar. Together, these results suggest that phosphorylation of the XCds1 SQ sites is not required for phosphorylation of other XCds1 sites, including the T355 and T359 autophosphorylation sites that are associated with complete XCds1 checkpoint-induced shifting. In contrast, the XCds1 S39A mutant is partially defective in its checkpoint-dependent response. The gel mobility shifting of the XCds1 S39A mutant is reproducibly delayed and reduced compared to the shifting of the WT or the 3AQ mutant construct (Fig. 5B, third part). The defect in the checkpoint-dependent gel mobility shift of the XCds1 4A mutant, in which all four PIKK phosphorylation sites are mutated to alanine, is even more pronounced, suggesting that the additional loss of phosphorylation at the SQ sites exacerbates the checkpoint defect of the XCds1 S39A mutant (Fig. 5B, bottom part). Thus, the combined phosphorylation of both the SQ and serine 39 sites in the XCds1 SCD is essential for the checkpoint-dependent gel mobility shifting of XCds1. Furthermore, in conjunction with the lack of gel mobility shifting of the XCds1 N86 S39A mutant fragment (Fig. 4D), these results suggest that phosphorylation of serine 39 is a critical event in the complete modification of XCds1.

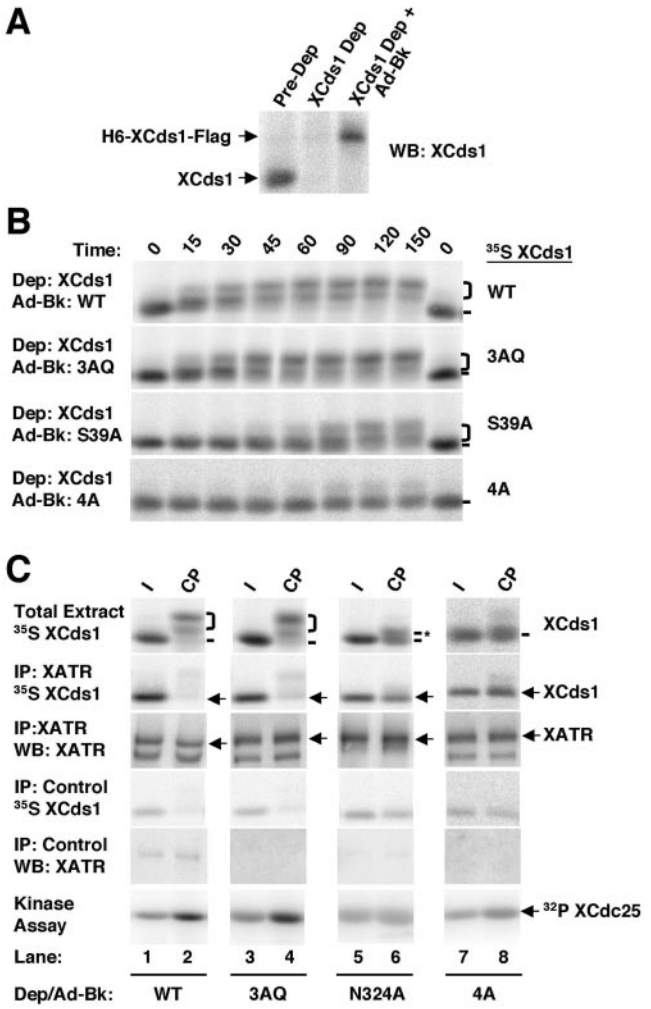

FIG. 5. Checkpoint-induced phosphorylation of the four PIKK sites is required for the activation of XCds1 and for dissociation of Cds1 from XATR. (A) *Xenopus* extracts were subjected to depletion of endogenous XCds1 and add back of recombinant XCds1 as described for Fig. 3B. (B) Mutations of 3AQ, S39A, and all four PIKK sites (4A) have slight, intermediate, and severe effects, respectively, on the full checkpoint-induced XCds1 gel mobility shift (bracket) that is indicative of Cds1 activation. The WT and mutant (3AQ, S39A, or 4A) forms of recombinant XCds1 were used to replace the endogenous XCds1 in depletion (Dep)–add-back (Ad-Bk) experiments performed as described for Fig. 3C. (C) Mutation of all four PIKK sites prevents dissociation of XCds1 from XATR during a checkpoint response and XCds1 activation. The indicated WT and mutant (3AQ, N324A, 4A) forms of recombinant XCds1 were used to replace the endogenous XCds1 in depletion–add-back experiments. These extracts were cycled as interphase (I) or dsDNA end checkpoint (CP) extracts and then subjected to association-dissociation analysis as described for Fig. 1C. Additionally, XCds1 immunoprecipitation and in vitro kinase assays (kinase assay) were performed as described for Fig. 3D.

We then went on to determine whether the direct phosphor-

ylation of the XCds1 amino terminus by the checkpoint PIKKs is also responsible for the checkpoint-induced dissociation between XCds1 and XATR (Fig. 5C, top and middle parts). As in the previous set of experiments, these experiments were performed with XCds1 mutant extracts that were prepared by depleting endogenous XCds1 and replacing it with various recombinant forms of XCds1; however, in this case, the XCds1 depletion–add-back extracts were either cycled as interphase or checkpoint extracts. We then subjected these to XATR or control immunoprecipitation as described previously (Fig. 1C). Both WT XCds1 and the 3AQ mutant associate with XATR in a checkpoint-sensitive manner, similar to endogenous XCds1 (Fig. 5C, compare to Fig. 1B). In both cases, XCds1 associates with the ATR-containing complex under interphase conditions (Fig. 5C, lanes 1 and 3) and dissociates from the complex upon checkpoint activation (Fig. 5C, lanes 2 and 4).

The kinase-dead XCds1 N324A mutant also associates with XATR in interphase extracts (Fig. 5C, lane 5). However, in the checkpoint extract the dissociation of the kinase-defective XCds1 mutant from the XATR complex was compromised, with a significant amount of XCds1 remaining associated with XATR (Fig. 5C, lane 6). This result indicates that XCds1 activity is required during a checkpoint response to induce complete dissociation of XCds1 from the XATR complex. However, it is interesting that the XCds1 mutant underwent a partial, minor gel mobility shift in the checkpoint extract (Fig. 5C, lane 6, total-extract lanes, line with asterisk), and the shifted form of XCds1 preferably dissociates from XATR in the checkpoint extract while the unshifted fraction remained associated (Fig. 5C, lane 6, compare the two migrating species of XCds1 N324A in the total extract to those that coprecipitate with XATR). As shown in Fig. 3C, kinase-dead XCds1 does not undergo a major checkpoint-dependent gel mobility shift in an extract background that lacks XCds1 activity. This major shift is observed in the WT and 3AQ depletion–add-back experiments (lanes 1 to 4) and is associated with complete XCds1 activation due to XCds1 autophosphorylation (Fig. 5C, kinase assay) (20). Instead, the XCds1 kinase-dead mutant displays only the minor shift due to phosphorylation of the XCds1 SCD. This result suggests that the checkpoint-induced phosphorylations on the amino terminus of XCds1 not only promotes XCds1 activation but also appears to play a direct role in inducing the dissociation of XCds1 from the XATR complex.

To test this possibility, we performed the depletion–add-back experiment with a full-length XCds1 mutant that cannot be modified, XCds1 3AQ, S39A (4A), and asked if it would associate and dissociate from the ATR complex. The XCds1 4A mutant fails to undergo significant checkpoint-dependent modification, as determined by the lack of a gel mobility shift (Fig. 5C, total-extract lanes 7 and 8). Significantly, this mutant coimmunoprecipitates with the ATR complex under both interphase and checkpoint conditions (ATR IP, Fig. 5C, lanes 7 and 8). Taken together, these results indicate that the dissociation of XCds1 from the ATR-containing complex requires phosphorylation of the SCD of XCds1. Furthermore, while XCds1 activity is needed for efficient dissociation, the phosphorylation of sites in the SCD alone promotes some degree of checkpoint-induced dissociation.

Finally, we investigated whether SCD phosphorylation is required for checkpoint-mediated activation of XCds1. Similar to the results shown in Fig. 3D, WT, but not kinase-dead (N324A), XCds1 is activated twofold during the checkpoint response (Fig. 5C, kinase assay, lanes 1 and 2 and lanes 5 and 6). In addition, the mutant XCds1 protein that lacks the three SQ phosphorylation sites (3AQ) undergoes nearly WT levels of activation (1.9-fold; Fig. 5C, kinase assay, lanes 3 and 4). This result is consistent with the nearly WT levels of shifting observed with this mutant (Fig. 5B and C). Conversely, the 4A mutant that lacks all of the SCD phosphorylation sites is poorly activated during the checkpoint response (1.3-fold; Fig. 5C, kinase assay, lanes 7 and 8). Again, this result is consistent with the deficient shifting of this mutant (Fig. 5B and C). Thus, mutant XCds1 proteins that cannot be phosphorylated in the SCD fail to shift, dissociate from ATR, or get activated during a checkpoint response.

ATR, ATM, and DNA-PK phosphorylate XCds1 with different specificities. We next sought to identify the kinase(s) responsible for the phosphorylation of the XCds1 SQ motifs and serine 39 during a checkpoint response. Although XCds1 phosphorylates other sites in XCds1 (T355 and T359) (Fig. 3), it does not phosphorylate any sites in the amino-terminal 86-amino-acid fragment of XCds1 (data not shown). The wortmannin sensitivity and the identity of the phosphorylated sites suggest that the checkpoint PIKKs (ATM, ATR, and/or DNA-PK) might be responsible for this phosphorylation. To test this, we asked whether the checkpoint PIKKs could phosphorylate the amino terminus of XCds1 in vitro. Antibodies against XATR and XATM were used to immunoprecipitate these two checkpoint kinases from *Xenopus* extracts (Fig. 6A). Both XATR and XATM phosphorylate recombinant GST fusions of Xp53, human BRCA1, and *Xenopus* Chk1 in an SQ-specific and caffeine-sensitive manner, indicating that these immunoprecipitated kinases are functional (data not shown).

We next examined the ability of XATM and XATR to phosphorylate the amino terminus of human Cds1, which has been previously shown to be a substrate for human ATR and ATM (4, 39, 41). Both XATR and XATM phosphorylate the WT hCds1 fusion protein (Fig. 6B). Furthermore, as in the case of human ATR and ATM, XATR and XATM phosphorylate the hCds1 threonine 68 mutant (T68A) less efficiently than the WT hCds1 fragment (WT). Thus, the high specificity for the hCds1 T68 site is conserved between human ATR and XATR and human ATM and XATM.

We then tested XATM and XATR for the ability to phosphorylate XCds1. In contrast to control immunoprecipitations, both kinases phosphorylate the XCds1 N86 WT fragment efficiently (Fig. 6C). However, while mutation of the three SQ sites (3AQ) significantly reduces that ability of XATR to phosphorylate the N86 fragment (80% reduction), the same mutation has little effect on the level of XATM-mediated phosphorylation (25% reduction). We observed a similar lack of SQ specificity when we performed in vitro kinase assays with recombinant human ATM and the XCds1 3AQ substrate, suggesting that the SQ-independent phosphorylation is not due to contaminants in the XATM IP (data not shown). Finally, we found that both XATM and XATR appear to be unable to phosphorylate serine 39, because mutation of this site in combination with the 3AQ mutation (4A) did not reduce further the phosphorylation of the XCds1 fragment by either kinase (Fig. 6C). Together, these results suggest that XATR is a

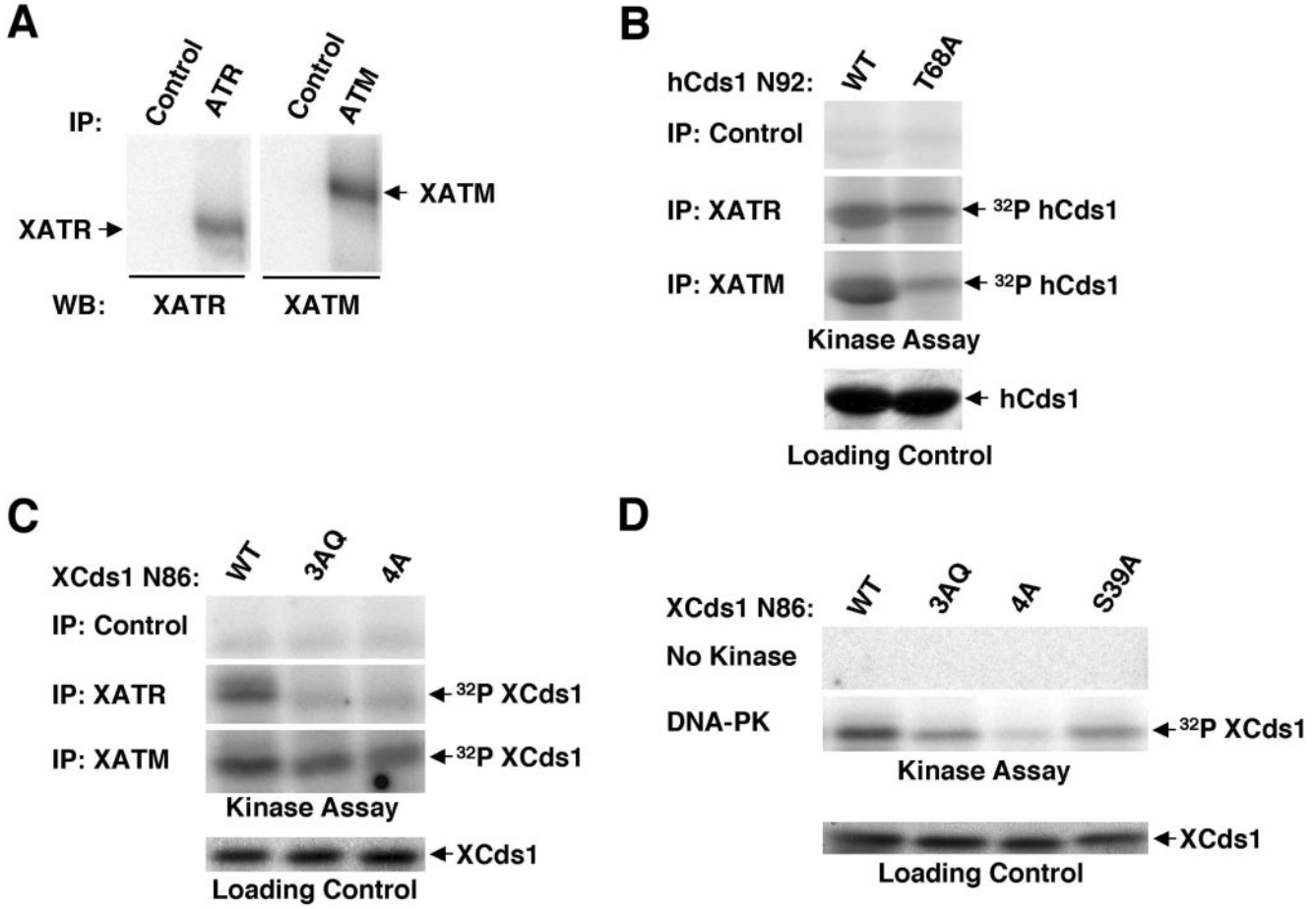

FIG. 6. ATR, ATM, and DNA-PK phosphorylate XCds1 with different specificities. (A) XATR and XATM were immunoprecipitated from *Xenopus* egg extracts and either subjected to Western blot (WB) analysis with the respective antibodies or used in in vitro kinase assays (B and C). (B) XATR and ATM possess kinase specificity similar to that of human ATR and ATM, preferentially phosphorylating threonine 68 of hCds1. (Top [kinase assay]) Immunoprecipitated control, XATR, and XATM were used in in vitro kinase assays with a GST fusion of the first 92 amino acids of hCds1 as the substrate. This substrate was either WT or mutated so that the TQ at position 68 was changed to AQ (T68A). (Bottom [loading control]) Coomassie staining shows that equal amounts of the hCds1 substrates were used. (C) XATR and XATM phosphorylate XCds1 on SQ sites but not on serine 39. (Top [kinase assay]) Immunoprecipitated control, XATR, and XATM were used in in vitro kinase assays with a GST fusion of the first 86 amino acids of XCds1 as the substrate. This substrate was either WT or mutated so that the three SQ sites were changed to AQ (3AQ) or so that the 3AQ mutant was combined with an S39A substitution (4A). (Bottom [loading control]) Coomassie staining shows that equal amounts of the XCds1 substrates were used. (D) DNA-PK phosphorylates XCds1 on serine 39 and SQ sites. (Top [kinase assay]) The same XCds1 substrates used in panel C and an S39A XCds1 mutation were used in in vitro kinase assays with human DNA-PK as the kinase. (Bottom [loading control]) Coomassie staining shows that equal amounts of the XCds1 substrates were used.

candidate kinase that can phosphorylate the three SQ sites of XCds1. Furthermore, while XATM can phosphorylate the first 86 amino acids of XCds1, most of this phosphorylation is at some other, non-SQ, site(s). Finally, both XATR and XATM are unlikely candidates for the checkpoint-dependent phosphorylation of XCds1 serine 39.

In general, the checkpoint PIKKs (ATR, ATM, and DNA-PK) have been shown to exhibit strict phosphorylation site specificity in vitro, requiring SQ/TQ motifs for phosphorylation (1, 29). However, DNA-PK has been shown to exhibit a higher degree of flexibility in its phosphorylation site preference in vivo (13). While DNA-PK has not been previously implicated in Cds1 regulation, this PIKK is involved with various cell cycle checkpoint components (19, 59). We used recombinant human DNA-PK for our studies. DNA-PK efficiently phosphorylates a WT Xp53 fragment but not an SQ mutant fragment (S14A) of Xp53, showing that this human kinase phosphorylates a *Xenopus* checkpoint substrate with conserved specificity (data not shown). As with XATR and XATM, DNA-PK phosphorylates XCds1 N86 WT effectively, and as with XATR, mutation of the three SQ sites (3AQ) diminishes phosphorylation to 40% of WT levels. However, in contrast to XATR and XATM, the additional mutation of S39 to alanine (4A) causes a significant reduction in phosphorylation (10% compared to that of the WT, Fig. 6D). Furthermore, mutation of the serine 39 site alone (S39A) reduces the level of phosphorylation compared to that of the WT fragment (60% reduction). These results suggest that DNA-PK is the wortmannin-sensitive kinase responsible for serine 39 phosphorylation during a checkpoint response. In sum, all three checkpoint PIKKs, ATM, ATR, and DNA-PK, can phosphorylate XCds1 in vitro. However, only DNA-PK can phosphorylate XCds1 on serine 39.

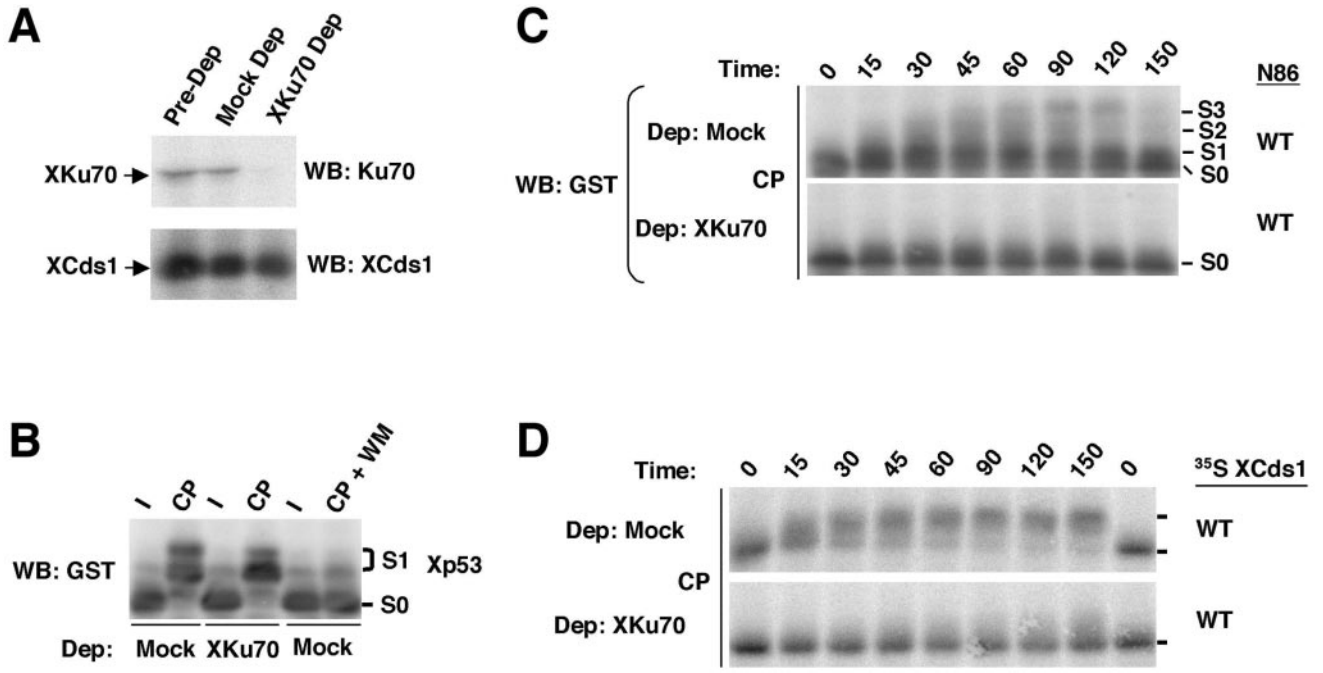

FIG. 7. Depletion of the DNA-PK subunit XKu70 impairs checkpoint (CP)-dependent phosphorylation of the XCds1 SCD and phosphorylation of full-length XCds1 that is indicative of activation. (A) XKu70 is specifically depleted from extracts. *Xenopus* extract was subject to XKu70 (XKu70 Dep) or control antibody (Mock Dep) depletion. Samples of the predepletion, mock depletion, and XKu70 postdepletion extracts were analyzed by Western blotting (WB) with anti-Ku70 and anti-XCds1 antibodies. (B) The CP-dependent, wortmannin (WM)-sensitive shifting of GST-Xp53 N39 is not affected by XKu70 depletion. GST-Xp53 N39 (Xp53) was added to mock- or XKu70-depleted extracts and then cycled as interphase (I) or dsDNA end CP extracts either with or without WM. Samples were taken at 120 min and processed as described for Fig. 4B. Shifts are indicated by S0 and S1. (C) Depletion of XKu70 eliminates the CP-dependent gel mobility shifting of the GST-XCds1 N86 fragment. GST-XCds1 N86 (WT) was added to mock- or XKu70-depleted dsDNA end CP extracts. Samples were taken at the indicated times and processed as described for Fig. 4B. (D) XKu70 depletion eliminates the CP-dependent gel mobility shifting of full-length XCds1. Full-length, ^{35}S-labeled XCds1 (WT) was added to mock- or XKu70-depleted dsDNA end CP extracts. Samples were taken at the indicated times and processed as described for Fig. 3.

Depletion of *Xenopus* Ku70 disrupts checkpoint-dependent phosphorylation and activation of XCds1. DNA-PK is a heterotrimeric complex consisting of DNA-PK, Ku70, and Ku80; all subunits are required for catalytic activity (48). Therefore, to further explore the role of DNA-PK in the regulation of XCds1, we removed the DNA-PK activity by depleting *Xenopus* Ku70 (XKu70) from *Xenopus* extracts (32). Immunodepletion of XKu70 effectively removed XKu70, but not XCds1, from the extract (Fig. 7A). To confirm that depletion of XKu70 does not disrupt the overall checkpoint response, we examined the gel mobility shifting of Xp53 in XKu70-depleted extracts. Like human p53, Xp53 is multiply phosphorylated in a checkpoint-dependent fashion. For example, the amino terminus of Xp53 has a potential PIKK phosphorylation site (SQ) and is phosphorylated in a dsDNA checkpoint-dependent manner, directly and/or indirectly, by ATR, ATM, and/or DNA-PK (17) (Fig. 7B; data not shown). We observed that the phosphorylation of an amino-terminal Xp53 GST fusion protein (GST-Xp53 N39) in *Xenopus* dsDNA end checkpoint extracts results in a gel mobility shift. Furthermore, GST-Xp53 N39 undergoes equal levels of checkpoint-dependent gel mobility shifting in mock-depleted and XKu70-depleted extracts, suggesting that at least some aspects of the checkpoint response remain intact. Finally, although depletion of XKu70 has little effect on the checkpoint-induced shifting of Xp53, this shift is wortmannin sensitive. Together, these results suggest that XATR and/or XATM are functional in XKu70-depleted extracts.

We then examined the gel mobility shifting of the amino-terminal GST-XCds1 N86 fragment in these depleted extracts. Strikingly, depletion of XKu70 disrupts the checkpoint-dependent gel mobility shift of the XCds1 fragment (Fig. 7C, compare mock- and Ku70-depleted parts). This result is comparable to the loss of shifting observed with the GST-XCds1 N86 S39A fragment (Fig. 4D). Together, these results suggest that *Xenopus* DNA-PK is responsible for the phosphorylation of XCds1 on serine 39.

Finally, we asked whether depletion of XKu70 had any effect on the complete shifting of full-length XCds1 that is associated with XCds1 activation. Compared to that of the mock-depleted control, depletion of XKu70 leads to loss of full-length XCds1 checkpoint-dependent shifting (Fig. 7D) and suggests that in the absence of Ku70, XCds1 cannot be activated. Thus, DNA-PK plays an essential function in the dsDNA end checkpoint response by inducing XCds1 modification and activation in *Xenopus* extracts.

Different regions within the XCds1 FHA domain have distinct functions in XCds1 activation and XATR association. The results presented so far suggest two possible mechanisms of XCds1 activation. The first possibility is that phosphorylation of XCds1 by the checkpoint PIKKs leads to dissociation

from the XATR-containing complex and that this allows for subsequent XCds1 activation by autophosphorylation. The second possibility is that these PIKK-mediated phosphorylations of XCds1 have a direct role in activating XCds1 and are required for XCds1 activation independent of their role in promoting the disassociation between XATR and XCds1. To examine these two possibilities, we sought to better understand the molecular nature of the interaction between XCds1 and XATR. First, we focused on the XCds1 FHA domain. This domain has been shown to participate in protein-protein interactions, principally through their association with phosphorylated threonine residues (36). The hCds1 FHA domain has been implicated by a number of groups as being involved in self-activation of hCds1 via dimerization (2, 3, 47, 58). Second, when we examined the amino-terminal portion of the XCds1 FHA domain, we noticed a proline-rich region highlighted by the presence of a putative SH3 domain binding site, identified by the residues PXXP (prolines 52 and 55, Fig. 2A). A similar site has been noted, but not tested, in the FHA domain of hCds1 (10). Although XATR does not possess an SH3 domain, it is possible that the association between XATR and XCds1 is indirect, mediated by SH3 domain-possessing adaptor proteins.

We prepared two mutant XCds1 proteins. The first, XCds1 R117W, contains a mutation analogous to an hCds1 mutation (R145W) that is associated with Li-Fraumeni syndrome and colon cancer and putatively disrupts the hCds1 FHA domain (7, 35, 36). The second, XCds1 P55A, disrupts the potential XCds1 SH3 domain binding site. In vitro, XCds1 P55A possesses basal kinase activity, suggesting that the mutation does not disrupt the kinase function of XCds1 (Fig. 2C). On the other hand, the XCds1 R117W mutant has negligible kinase activity in vitro, indicating that this mutation causes loss of XCds1 kinase function, as well as disrupting the putative FHA domain (Fig. 2C). When XCds1 depletion–add-back checkpoint extracts were supplied with the recombinant XCds1 R117W mutant, the gel mobility shift of this mutant was significantly delayed and reduced (Fig. 8A). In contrast, when similar experiments were performed with the recombinant XCds1 P55A mutant, this construct underwent a checkpoint-dependent gel mobility shift similar to that of WT XCds1. Consistent with these shifting results, in vitro kinase assays with recombinant XCds1 recovered from interphase or checkpoint extracts indicate that while XCds1 R117W fails to become activated, the XCds1 P55A mutant experiences nearly WT levels of activation (1.8-fold) (Fig. 8B, kinase assay). Thus, the putative FHA domain, but not the putative SH3 binding domain, is required for the XCds1 activation in checkpoint-activated extracts.

We next examined the ability of the putative FHA and SH3 binding domain mutants to associate with and dissociate from the XATR-containing complex. The XCds1 R117W mutant associates with the ATR complex in interphase but does not dissociate from it under checkpoint conditions (Fig. 8B, middle parts, lanes 1 and 2). Thus, although this FHA domain mutation disrupts XCds1 kinase activity and impairs the ability of XCds1 to become activated during a checkpoint response, it does not appear to affect the interaction between XCds1 and XATR. In contrast, the XCds1 P55A mutant, which is activated in a checkpoint-dependent manner similarly to the WT, failed to associate with XATR under any of the cell cycle

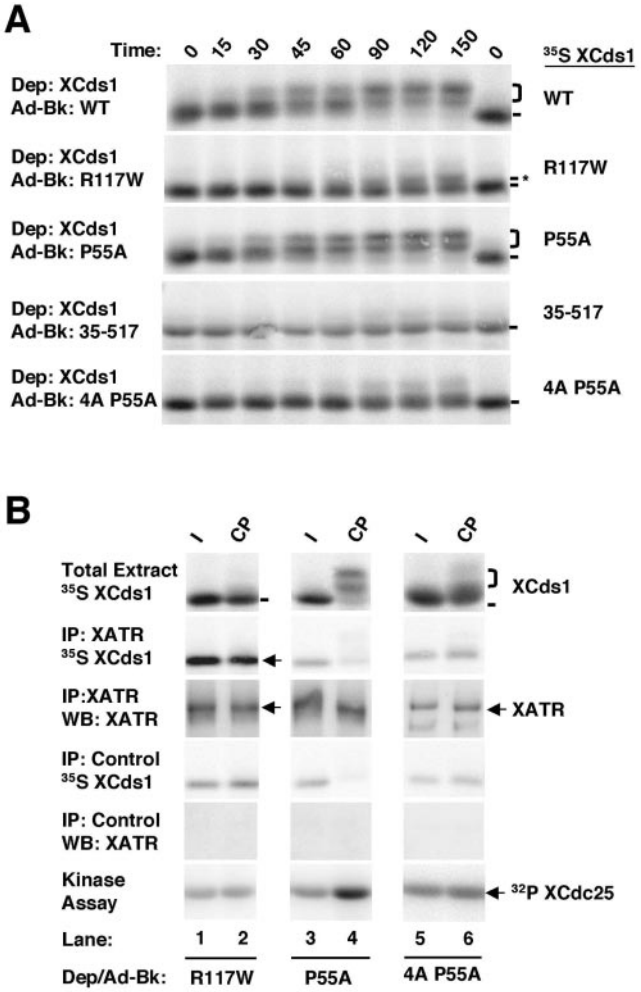

FIG. 8. Different regions within the XCds1 FHA domain have distinct functions in XCds1 shifting, activation, and dissociation. (A) While mutation of the SH3 domain binding site (P55A) has little effect on the shifting of full-length XCds1, mutation of the FHA domain (R117W), loss of the SCD (35-517), or combination of the SH3 domain binding site mutation with the PIKK phosphorylation site mutations largely eliminates this shift. Depletion–add-back experiments were done as described for Fig. 5B. Labels are as in Fig. 3A. (B) The R117W mutation blocks the checkpoint-induced dissociation, while the P55A and 4A P55A mutations block the association under all conditions, of XCds1 with XATR-containing complexes. Additionally, in vitro kinase assays indicate that only the P55A can be activated by dsDNA end checkpoints. Experiments were performed as described for Fig. 3D and 5C.

condition tested (Fig. 8B, middle parts, lanes 3 and 4, compare the level of [^{35}S]XCds1 in the control IP to the level in the ATR IP). These results suggest that the putative XCds1 SH3 binding domain, but not the FHA domain, plays a critical role in XCds1-XATR association. Additionally, since the XCds1 P55A mutant undergoes a WT-like gel mobility shift and activation in checkpoint extracts, the association with the XATR complex does not appear to be required for XCds1 activation during the checkpoint response.

Phosphorylation of the amino-terminal SCD activates XCds1. PIKK-mediated phosphorylation of XCds1 is required for the dissociation of XCds1 from XATR-containing complexes and

for the complete activation of XCds1 (Fig. 1E and 5B and C). This led us to ask by what mechanism PIKK phosphorylation and subsequent dissociation promote complete XCds1 activation. It could be that the amino-terminal SCD of XCds1 functions as a negative regulator of XCds1 activation. As a negative regulator, this region could function by sequestering XCds1 in an ATR-containing complex under noncheckpoint conditions or it could function as an autoinhibitory region (AIR), similar to what has been observed with the regulatory domain of Chk1 (28). Alternatively, the PIKK phosphorylations may serve in a direct activation role. In this situation, covalent modification of the amino terminus of XCds1 during the checkpoint response would be required for subsequent activation independent of XATR association-dissociation.

To test these possibilities, we designed two types of XCds1 mutant constructs. The first was a deletion mutant that lacks the first 34 amino acids of XCds1 (XCds1 35-517). This construct possesses WT levels of basal kinase activity (Fig. 2C). When tested in a depletion–add-back experiment similar to that shown in Fig. 3C, the XCds1 35-517 deletion mutant failed to undergo any significant checkpoint-dependent gel mobility shift, suggesting that it is defective in checkpoint-dependent activation (Fig. 8A). Thus, it is unlikely that the amino-terminal region of XCds1 containing the SQ sites is an AIR. Instead, it appears that this region of XCds1 may play an active role in XCds1 checkpoint-dependent activation.

The second construct was a modification of the association-independent XCds1 P55A mutant. This modified mutant not only lacked the putative SH3 binding domain (P55A) but also the four PIKK phosphorylation sites (4A: 3AQ and S39A). In in vitro kinase assays, this XCds1 4A P55A mutant has basal kinase activity similar to that of the XCds1 P55A mutant (Fig. 2C). As predicted, the XCds1 4A P55A mutant, like the XCds1 P55A mutant, failed to associate with XATR under any of the cell cycle conditions tested in our deletion–add-back extracts (Fig. 8B, compare the level of [^{35}S]XCds1 in the control IP to that in the ATR IP). However, unlike the P55A mutant, the 4A P55A mutant has a reduced molecular weight shift and is poorly activated (1.3-fold) under checkpoint conditions (Fig. 8A and B, lower parts). Together, these results suggest that the amino terminus of XCds1 functions mechanistically as an activator and not as an inhibitor during the checkpoint response. Furthermore, phosphorylation of the amino terminus of XCds1 by the PIKKs is required not only for the dissociation of XCds1 from the complex but also for the direct activation of XCds1.

DISCUSSION

The link between defective checkpoint response pathways and an increased incidence of cancer highlights the need to maintain efficiently functioning checkpoint pathways. Of particular importance is the regulation of effectors of checkpoint responses such as the checkpoint kinase Cds1. This kinase modifies the activity of the cell cycle machinery through phosphorylation of key factors and is involved in all aspects of a checkpoint event: cell cycle arrest, DNA repair, and induction of apoptosis. Therefore, proper regulation of Cds1 function is essential to ensure timely and appropriate responses to a checkpoint signal.

In this work we show that three checkpoint PIKKs, XATM, XATR, and DNA-PK, are involved in XCds1 regulation during a checkpoint response. Interestingly, our data indicate that a complex including the checkpoint kinases XATR and XCds1 exists during an unperturbed cell cycle, an association that is mediated through a predicted SH3 domain binding region within XCds1. This association appears to be rapidly disrupted during specific checkpoint responses in which XCds1 is activated. Disruption of the XCds1-XATR association is driven in part by PIKK-mediated phosphorylation of multiple sites within the amino-terminal SCD of XCds1. Furthermore, phosphorylation of XCds1 on serine 39 by DNA-PK is essential for promoting XCds1-XATR dissociation and for inducing subsequent phosphorylation of XCds1 on amino-terminal SQ sites and kinase domain autophosphorylation sites. Together, these modifications lead to the activation of XCds1 during a checkpoint.

Like the activation of hCds1, it appears that the activation of XCds1 requires checkpoint PIKK activity. However, the lack of an analogous hCds1 threonine 68 residue suggests that XCds1 uses an alternative means of activation. Although the phosphorylation of XCds1 by the checkpoint PIKKs is an essential step in XCds1 activation, it is improbable that any of the resulting phosphorylated serines functions as a direct XCds1 FHA binding site. The XCds1 FHA domain is highly similar to that found in hCds1, particularly around residues that bind the phosphothreonine epitope (36). Thus, like its human counterpart, the XCds1 FHA domain is predicted to bind phosphothreonine, making it unlikely that any of the XCds1 serines phosphorylated by the checkpoint PIKKs would serve as a putative XCds1 FHA binding site. While our results do not allow us to formally eliminate this possibility, we hypothesize that the PIKK-mediated phosphorylations of XCds1 may play an alternative role during XCds1 activation. Although the phosphorylation of XCds1 serine 39 appears to be a critical event for XCds1 activation, the additional loss of phosphorylation on the XCds1 SQ sites seems to enhance the activation defect, suggesting that these phosphorylations may function in an additive manner. Together, phosphorylation of the four PIKK sites in XCds1 appears to directly induce dissociation from XATR, perhaps a required first step in XCds1 activation. However, dissociation is probably not the only function of these phosphorylations. Specifically, the 4A P55A XCds1 mutant that neither associates with ATR nor gets phosphorylated by the PIKKs fails to undergo activation during a checkpoint response. Thus, the phosphorylations of the XCds1 SCD seem to play dual roles: XCds1 release from the XATR complex and XCds1 activation.

Our results indicate that the amino terminus of XCds1 has an essential function during a checkpoint response. We examined the possibility that the XCds1 SCD has a negative regulatory function that is relieved by phosphorylation, similar to the AIR of Chk1 (28). However, when we tested an XCds1 SCD deletion construct (XCds1 35-517) in *Xenopus* checkpoint extracts, we found that this mutant failed to undergo the gel mobility shift that is associated with Cds1 activation, suggesting that this mutant is activation defective. This is the opposite of what would be predicted by removing an inhibitory domain. Instead, these results support the idea that when the XCds1 amino-terminal SCD is phosphorylated, it plays an activating role in XCds1 regulation.

Given the importance of human ATM kinase activity for the

activation of hCds1, the results of our in vitro kinase assays with *Xenopus* checkpoint PIKKs were intriguing. XATM exhibited a lack of SQ/TQ specificity when phosphorylating XCds1, phosphorylating the XCds1 3AQ mutant fragment only marginally less than the XCds1 WT construct. This is in contrast to XATR, in which mutation of the three XCds1 SQ motif serines nearly abolished the ability of XATR to phosphorylate XCds1. We are currently evaluating XCds1 for the presence of an additional XATM phosphorylation site(s) and the possible significance of these modifications in regard to XCds1 regulation.

The results indicating that DNA-PK is the kinase responsible for the phosphorylation of XCds1 serine 39 were also unexpected. Phosphorylation of the non-SQ serine 39 site in XCds1 appears to be a critical event in XCds1 activation, suggesting a function for DNA-PK in Cds1 activation not previously observed. Consistent with these results is the observation that XCds1 becomes activated during checkpoint responses induced by dsDNA ends, a checkpoint condition under which DNA-PK would also be active. An intriguing connection between these two checkpoint kinases is their involvement in p53-dependent apoptosis (8, 25, 57). While DNA-PK has not been shown to be involved in the regulation of hCds1, hCds1 does possess a residue analogous to XCds1 serine 39. Interestingly, a recent study suggests that hCds1 and DNA-PK function synergistically through a latent population of p53 to induce apoptosis in mouse embryo fibroblasts (26), linking the two kinases by function.

While our results indicate that XCds1 is a substrate of XATR, the association between these two checkpoint kinases is more complex than would be expected from a kinase-substrate interaction and suggests an additional form of regulation. We favor the hypothesis that the association between XATR and XCds1 is in the form of a multiprotein complex. The observation that the putative SH3 domain binding region of XCds1 is required for the interaction between XCds1 and XATR raises the possibility that XCds1 interacts with an SH3 domain-possessing protein. However, the absence of a predicted SH3 domain in XATR suggests that the XATR-XCds1 interaction may be indirect. Interestingly, recent studies have suggested a potential interaction between hCds1 and the SH3 domain-possessing tyrosine kinase c-Abl mediated by the checkpoint protein BRCA1. BRCA1 has been shown to interact in vivo with both hCds1 and c-Abl, suggesting a common intermediate for these checkpoint kinases (16, 34). It is worth noting that the associations between BRCA1 and hCds1 and BRCA1 and c-Abl are disrupted during cell cycle checkpoints, similar to what we observed with the interaction between XATR and XCds1. However, an interaction between Cds1 and c-Abl has not yet been shown experimentally. The involvement of multiple regions of the Cds1 FHA domain in protein-protein interactions is not unprecedented. For example, BRCA1 has been shown to interact with hCds1 through multiple, distinct regions of the hCds1 FHA domain (36).

In a noncheckpoint situation, it would be essential for the cell to ensure that checkpoint kinases such as XCds1 are maintained in an inactive state to prevent interference with normal cell cycle progression. The association between XCds1 and this checkpoint complex may serve as a form of regulation. For example, a BRCA1 mutation that disrupts its ability to associate with c-Abl results in constitutively high levels of c-Abl activity (16). In a similar fashion, XCds1 may be kept in an inactive state, at least in part, through protein-protein interactions under normal cell cycle conditions.

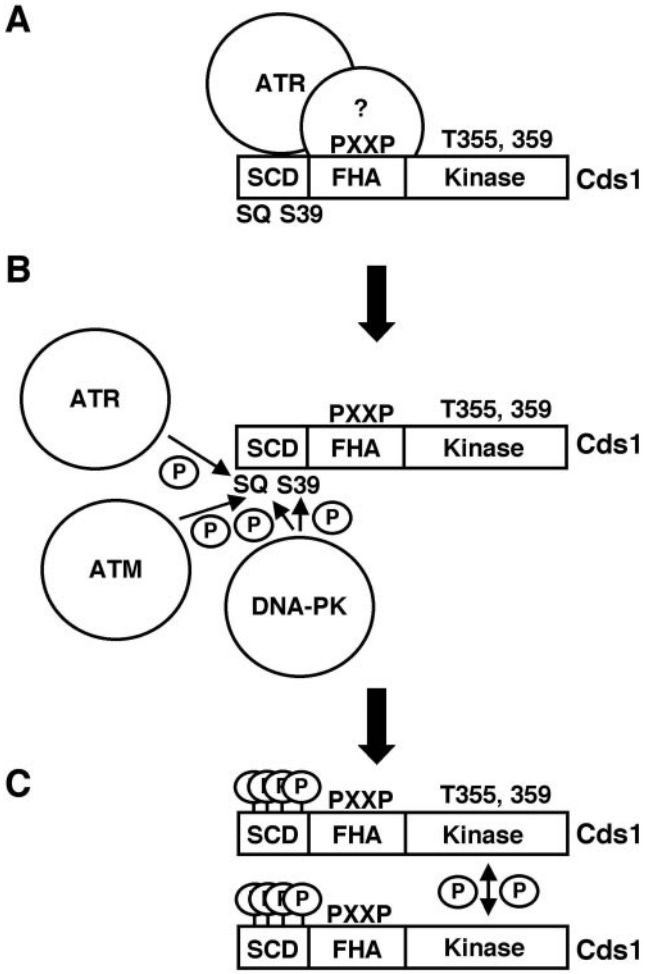

FIG. 9. Model of XCds1 regulation. (A) In an unperturbed cell cycle, XCds1 has low activity and is found in a complex with XATR and possibly other proteins. Formation of this complex requires an intact putative SH3 binding domain (PXXP) in XCds1. (B) Upon checkpoint induction, PIKKs phosphorylate the amino-terminal SCD of XCds1, first on serine 39 (within 7 min) and then on the remaining SQ sites. These phosphorylations promote the dissociation of XCds1 from the XATR-containing complex and cause a minor gel mobility shift of XCds1. (C) Full activation of XCds1 is mediated by autophosphorylation of XCds1 on the activation loop threonines (T355 and T359), and these phosphorylations cause the major gel mobility shift of XCds1.

On the basis of this work we propose a model detailing how the checkpoint kinase XCds1 is regulated during a checkpoint response in *Xenopus* cell extracts (Fig. 9). In an unperturbed cell cycle, XCds1 is found in a complex containing the checkpoint PIKK XATR and possibly other proteins. This association is mediated through a putative SH3 domain binding site within XCds1 (Fig. 9A). In response to DNA damage (ssDNA or dsDNA ends) the DNA damage checkpoint pathway is activated, leading to the phosphorylation of several key residues in the amino-terminal SCD of XCds1. First, serine 39 is phosphorylated by DNA-PK. The SQ sites are then phosphorylated by XATR, XATM, and/or DNA-PK. Together, these

phosphorylations perform the dual functions of inducing XCds1 release from the XATR-containing complex and promoting XCds1 activation (Fig. 9B). Although phosphorylation of the SCD is required for XCds1 activation independently of XATR release, autophosphorylation of activation loop threonines 355 and/or 359 is thought to be the key event in obtaining fully functional XCds1 (Fig. 9C). Activated XCds1 then proceeds with its function during a checkpoint response, phosphorylating multiple cell cycle and cell cycle checkpoint proteins.

ACKNOWLEDGMENTS

We thank members of the Mueller laboratory and D. Bishop, G. Greene, A. Kitazono, and D. Steiner for helpful comments on this work and critical reading of the manuscript. We thank P. Carpenter, W. Dunphy, S. Elledge, and C. McGowan for gifts of reagents and C. Kurlander and R. Relwani for technical assistance.

This work was supported by grants to P.R.M. from the National Institutes of Health (RO1 CA84007) and the Sidney Kimmel Foundation for Cancer Research and a translational research grant from the Ludwig Institute for Cancer Research. T.D.M. has been supported in part by a National Institutes of Health training grant (T32 GM07183). P.R.M. is a Kimmel Scholar.

REFERENCES

1. **Abraham, R. T.** 2001. Cell cycle checkpoint signaling through the ATM and ATR kinases. Genes Dev. **15:**2177–2196.
2. **Ahn, J., and C. Prives.** 2002. Checkpoint kinase 2 (Chk2) monomers or dimers phosphorylate Cdc25C after DNA damage regardless of threonine 68 phosphorylation. J. Biol. Chem. **277:**48418–48426.
3. **Ahn, J. Y., X. Li, H. L. Davis, and C. E. Canman.** 2002. Phosphorylation of threonine 68 promotes oligomerization and autophosphorylation of the Chk2 protein kinase via the forkhead-associated domain. J. Biol. Chem. **277:**19389–19395.
4. **Ahn, J. Y., J. K. Schwarz, H. Piwnica-Worms, and C. E. Canman.** 2000. Threonine 68 phosphorylation by ataxia telangiectasia mutated is required for efficient activation of Chk2 in response to ionizing radiation. Cancer Res. **60:**5934–5936.
5. **Alexandropoulos, K., G. Cheng, and D. Baltimore.** 1995. Proline-rich sequences that bind to Src homology 3 domains with individual specificities. Proc. Natl. Acad. Sci. USA **92:**3110–3114.
6. **Bartek, J., J. Falck, and J. Lukas.** 2001. CHK2 kinase—a busy messenger. Nat. Rev. Mol. Cell Biol. **2:**877–886.
7. **Bell, D. W., J. M. Varley, T. E. Szydlo, D. H. Kang, D. C. Wahrer, K. E. Shannon, M. Lubratovich, S. J. Verselis, K. J. Isselbacher, J. F. Fraumeni, J. M. Birch, F. P. Li, J. E. Garber, and D. A. Haber.** 1999. Heterozygous germ line hCHK2 mutations in Li-Fraumeni syndrome. Science **286:**2528–2531.
8. **Bharti, A., S. K. Kraeft, M. Gounder, P. Pandey, S. Jin, Z. M. Yuan, S. P. Lees-Miller, R. Weichselbaum, D. Weaver, L. B. Chen, D. Kufe, and S. Kharbanda.** 1998. Inactivation of DNA-dependent protein kinase by protein kinase Cδ: implications for apoptosis. Mol. Cell. Biol. **18:**6719–6728.
9. **Blasina, A., I. V. de Weyer, M. C. Laus, W. H. Luyten, A. E. Parker, and C. H. McGowan.** 1999. A human homologue of the checkpoint kinase Cds1 directly inhibits Cdc25 phosphatase. Curr. Biol. **9:**1–10.
10. **Brown, A. L., C. H. Lee, J. K. Schwarz, N. Mitiku, H. Piwnica-Worms, and J. H. Chung.** 1999. A human Cds1-related kinase that functions downstream of ATM protein in the cellular response to DNA damage. Proc. Natl. Acad. Sci. USA **96:**3745–3750.
11. **Carpenter, P. B., P. R. Mueller, and W. G. Dunphy.** 1996. Role for a *Xenopus* Orc2-related protein in controlling DNA replication. Nature **379:**357–360.
12. **Carr, A. M.** 1997. Control of cell cycle arrest by the Mec1sc/Rad3sp DNA structure checkpoint pathway. Curr. Opin. Genet. Dev. **7:**93–98.
13. **Chan, D. W., R. Ye, C. J. Veillette, and S. P. Lees-Miller.** 1999. DNA-dependent protein kinase phosphorylation sites in Ku 70/80 heterodimer. Biochemistry **38:**1819–1828.
14. **Elledge, S. J.** 1996. Cell cycle checkpoints: preventing an identity crisis. Science **274:**1664–1672.
15. **Falck, J., C. Lukas, M. Protopopova, J. Lukas, G. Selivanova, and J. Bartek.** 2001. Functional impact of concomitant versus alternative defects in the Chk2-p53 tumour suppressor pathway. Oncogene **20:**5503–5510.
16. **Foray, N., D. Marot, V. Randrianarison, N. D. Venezia, D. Picard, M. Perricaudet, V. Favaudon, and P. Jeggo.** 2002. Constitutive association of BRCA1 and c-Abl and its ATM-dependent disruption after irradiation. Mol. Cell. Biol. **22:**4020–4032.
17. **Giaccia, A. J., and M. B. Kastan.** 1998. The complexity of p53 modulation: emerging patterns from divergent signals. Genes Dev. **12:**2973–2983.
18. **Gotoh, T., K. Ohsumi, T. Matsui, H. Takisawa, and T. Kishimoto.** 2001. Inactivation of the checkpoint kinase Cds1 is dependent on cyclin B-Cdc2 kinase activation at the meiotic G_2/M-phase transition in *Xenopus* oocytes. J. Cell Sci. **114:**3397–3406.
19. **Goudelock, D. M., K. Jiang, E. Pereira, B. Russell, and Y. Sanchez.** 2003. Regulatory interactions between the checkpoint kinase Chk1 and the proteins of the DNA-dependent protein kinase complex. J. Biol. Chem. **278:**29940–29947.
20. **Guo, Z., and W. G. Dunphy.** 2000. Response of *Xenopus* Cds1 in cell-free extracts to DNA templates with double-stranded ends. Mol. Biol. Cell **11:**1535–1546.
21. **Guo, Z., A. Kumagai, S. X. Wang, and W. G. Dunphy.** 2000. Requirement for Atr in phosphorylation of Chk1 and cell cycle regulation in response to DNA replication blocks and UV-damaged DNA in *Xenopus* egg extracts. Genes Dev. **14:**2745–2756.
22. **Hekmat-Nejad, M., Z. You, M. C. Yee, J. W. Newport, and K. A. Cimprich.** 2000. *Xenopus* ATR is a replication-dependent chromatin-binding protein required for the DNA replication checkpoint. Curr. Biol. **10:**1565–1573.
23. **Higuchi, R., B. Krummel, and R. K. Saiki.** 1988. A general method of *in vitro* preparation and specific mutagenesis of DNA fragments: study of protein and DNA interactions. Nucleic Acids Res. **16:**7351–7367.
24. **Hirao, A., A. Cheung, G. Duncan, P. M. Girard, A. J. Elia, A. Wakeham, H. Okada, T. Sarkissian, J. A. Wong, T. Sakai, E. De Stanchina, R. G. Bristow, T. Suda, S. W. Lowe, P. A. Jeggo, S. J. Elledge, and T. W. Mak.** 2002. Chk2 is a tumor suppressor that regulates apoptosis in both an ataxia telangiectasia mutated (ATM)-dependent and an ATM-independent manner. Mol. Cell. Biol. **22:**6521–6532.
25. **Hirao, A., Y. Y. Kong, S. Matsuoka, A. Wakeham, J. Ruland, H. Yoshida, D. Liu, S. J. Elledge, and T. W. Mak.** 2000. DNA damage-induced activation of p53 by the checkpoint kinase Chk2. Science **287:**1824–1827.
26. **Jack, M. T., R. A. Woo, N. Motoyama, H. Takai, and P. W. Lee.** 2004. DNA-dependent protein kinase and checkpoint kinase 2 synergistically activate a latent population of p53 upon DNA damage. J. Biol. Chem. **279:**15269–15273.
27. **Jones, R. E., J. R. Chapman, C. Puligilla, J. M. Murray, A. M. Car, C. C. Ford, and H. D. Lindsay.** 2003. XRad17 is required for the activation of XChk1 but not XCds1 during checkpoint signaling in *Xenopus*. Mol. Biol. Cell **14:**3898–3910.
28. **Katsuragi, Y., and N. Sagata.** 2004. Regulation of Chk1 kinase by autoinhibition and ATR-mediated phosphorylation. Mol. Biol. Cell **15:**1680–1689.
29. **Kim, S. T., D. S. Lim, C. E. Canman, and M. B. Kastan.** 1999. Substrate specificities and identification of putative substrates of ATM kinase family members. J. Biol. Chem. **274:**37538–37543.
30. **Kumagai, A., and W. G. Dunphy.** 1995. Control of the Cdc2/cyclin B complex in *Xenopus* egg extracts arrested at a G_2/M checkpoint with DNA synthesis inhibitors. Mol. Biol. Cell **6:**199–213.
31. **Kumagai, A., Z. Guo, K. H. Emami, S. X. Wang, and W. G. Dunphy.** 1998. The *Xenopus* Chk1 protein kinase mediates a caffeine-sensitive pathway of checkpoint control in cell-free extracts. J. Cell Biol. **142:**1559–1569.
32. **Labhart, P.** 1999. Ku-dependent nonhomologous DNA end joining in *Xenopus* egg extracts. Mol. Cell. Biol. **19:**2585–2593.
33. **Lee, C. H., and J. H. Chung.** 2001. The hCds1 (Chk2)-FHA domain is essential for a chain of phosphorylation events on hCds1 that is induced by ionizing radiation. J. Biol. Chem. **276:**30537–30541.
34. **Lee, J. S., K. M. Collins, A. L. Brown, C. H. Lee, and J. H. Chung.** 2000. hCds1-mediated phosphorylation of BRCA1 regulates the DNA damage response. Nature **404:**201–204.
35. **Lee, S. B., S. H. Kim, D. W. Bell, D. C. Wahrer, T. A. Schiripo, M. M. Jorczak, D. C. Sgroi, J. E. Garber, F. P. Li, K. E. Nichols, J. M. Varley, A. K. Godwin, K. M. Shannon, E. Harlow, and D. A. Haber.** 2001. Destabilization of CHK2 by a missense mutation associated with Li-Fraumeni syndrome. Cancer Res. **61:**8062–8067.
36. **Li, J., B. L. Williams, L. F. Haire, M. Goldberg, E. Wilker, D. Durocher, M. B. Yaffe, S. P. Jackson, and S. J. Smerdon.** 2002. Structural and functional versatility of the FHA domain in DNA-damage signaling by the tumor suppressor kinase Chk2. Mol. Cell **9:**1045–1054.
37. **Lou, Z., K. Minter-Dykhouse, X. Wu, and J. Chen.** 2003. MDC1 is coupled to activated CHK2 in mammalian DNA damage response pathways. Nature **421:**957–961.
38. **Matsuoka, S., M. Huang, and S. J. Elledge.** 1998. Linkage of ATM to cell cycle regulation by the Chk2 protein kinase. Science **282:**1893–1897.
39. **Matsuoka, S., G. Rotman, A. Ogawa, Y. Shiloh, K. Tamai, and S. J. Elledge.** 2000. Ataxia telangiectasia-mutated phosphorylates Chk2 *in vivo* and *in vitro*. Proc. Natl. Acad. Sci. USA **97:**10389–10394.
40. **McGowan, C. H.** 2002. Checking in on Cds1 (Chk2): a checkpoint kinase and tumor suppressor. Bioessays **24:**502–511.
41. **Melchionna, R., X. B. Chen, A. Blasina, and C. H. McGowan.** 2000. Threonine 68 is required for radiation-induced phosphorylation and activation of Cds1. Nat. Cell Biol. **2:**762–765.
42. **Mueller, P. R., T. R. Coleman, and W. G. Dunphy.** 1995. Cell cycle regulation of a *Xenopus* Wee1-like kinase. Mol. Biol. Cell **6:**119–134.
43. **Murray, A. W.** 1991. Cell cycle extracts. Methods Cell Biol. **36:**581–605.

44. **Obenauer, J. C., L. C. Cantley, and M. B. Yaffe.** 2003. Scansite 2.0: proteome-wide prediction of cell signaling interactions using short sequence motifs. Nucleic Acids Res. **31:**3635–3641.
45. **Rhind, N., and P. Russell.** 2000. Chk1 and Cds1: linchpins of the DNA damage and replication checkpoint pathways. J. Cell Sci. **113**(Pt. 22)**:**3889–3896.
46. **Robertson, K., C. Hensey, and J. Gautier.** 1999. Isolation and characterization of *Xenopus* ATM (X-ATM): expression, localization, and complex formation during oogenesis and early development. Oncogene **18:**7070–7079.
47. **Schwarz, J. K., C. M. Lovly, and H. Piwnica-Worms.** 2003. Regulation of the Chk2 protein kinase by oligomerization-mediated cis- and trans-phosphorylation. Mol. Cancer Res. **1:**598–609.
48. **Smith, G. C., and S. P. Jackson.** 1999. The DNA-dependent protein kinase. Genes Dev. **13:**916–934.
49. **Stevens, C., L. Smith, and N. B. La Thangue.** 2003. Chk2 activates E2F-1 in response to DNA damage. Nat. Cell Biol. **5:**401–409.
50. **Stokes, M. P., R. Van Hatten, H. D. Lindsay, and W. M. Michael.** 2002. DNA replication is required for the checkpoint response to damaged DNA in *Xenopus* egg extracts. J. Cell Biol. **158:**863–872.
51. **Tanaka, K., and P. Russell.** 2001. Mrc1 channels the DNA replication arrest signal to checkpoint kinase Cds1. Nat. Cell Biol. **3:**966–972.
52. **Theard, D., M. Coisy, B. Ducommun, P. Concannon, and J. M. Darbon.** 2001. Etoposide and adriamycin but not genistein can activate the checkpoint kinase Chk2 independently of ATM/ATR. Biochem. Biophys. Res. Commun. **289:**1199–1204.
53. **Toh, G. W., and N. F. Lowndes.** 2003. Role of the Saccharomyces cerevisiae Rad9 protein in sensing and responding to DNA damage. Biochem. Soc. Trans. **31:**242–246.
54. **Turner, D. L., and H. Weintraub.** 1994. Expression of achaete-scute homolog 3 in *Xenopus* embryos converts ectodermal cells to a neural fate. Genes Dev. **8:**1434–1447.
55. **Walworth, N. C.** 2000. Cell-cycle checkpoint kinases: checking in on the cell cycle. Curr. Opin. Cell Biol. **12:**697–704.
56. **Wang, B., S. Matsuoka, P. B. Carpenter, and S. J. Elledge.** 2002. 53BP1, a mediator of the DNA damage checkpoint. Science **298:**1435–1438.
57. **Wang, S., M. Guo, H. Ouyang, X. Li, C. Cordon-Cardo, A. Kurimasa, D. J. Chen, Z. Fuks, C. C. Ling, and G. C. Li.** 2000. The catalytic subunit of DNA-dependent protein kinase selectively regulates p53-dependent apoptosis but not cell-cycle arrest. Proc. Natl. Acad. Sci. USA **97:**1584–1588.
58. **Xu, X., L. M. Tsvetkov, and D. F. Stern.** 2002. Chk2 activation and phosphorylation-dependent oligomerization. Mol. Cell. Biol. **22:**4419–4432.
59. **Yang, J., Y. Yu, H. E. Hamrick, and P. J. Duerksen-Hughes.** 2003. ATM, ATR and DNA-PK: initiators of the cellular genotoxic stress responses. Carcinogenesis **24:**1571–1580.
60. **Yang, S., C. Kuo, J. E. Bisi, and M. K. Kim.** 2002. PML-dependent apoptosis after DNA damage is regulated by the checkpoint kinase hCds1/Chk2. Nat. Cell Biol. **4:**865–870.
61. **Zhou, B. B., and S. J. Elledge.** 2000. The DNA damage response: putting checkpoints in perspective. Nature **408:**433–439.